RESEARCH ARTICLE

Flavonols regulate root hair development by modulating accumulation of reactive oxygen species in the root epidermis

Sheena R. Gayomba and Gloria K. Muday*

ABSTRACT

Reactive oxygen species (ROS) are signaling molecules produced by tissue-specific respiratory burst oxidase homolog (RBOH) enzymes to drive development. In *Arabidopsis thaliana*, ROS produced by RBOHC was previously reported to drive root hair elongation. We identified a specific role for one ROS, H_2O_2, in driving root hair initiation and demonstrated that localized synthesis of flavonol antioxidants control the level of H_2O_2 and root hair formation. Root hairs form from trichoblast cells that express RBOHC and have elevated H_2O_2 compared with adjacent atrichoblast cells that do not form root hairs. The flavonol-deficient *tt4* mutant has elevated ROS in trichoblasts and elevated frequency of root hair formation compared with the wild type. The increases in ROS and root hairs in *tt4* are reversed by genetic or chemical complementation. Auxin-induced root hair initiation and ROS accumulation were reduced in an *rbohc* mutant and increased in *tt4*, consistent with flavonols modulating ROS and auxin transport. These results support a model in which localized synthesis of RBOHC and flavonol antioxidants establish patterns of ROS accumulation that drive root hair formation.

KEY WORDS: Flavonols, Root hair, *Arabidopsis*, ROS, Antioxidant

INTRODUCTION

Root hair formation follows an elegant developmental sequence controlled by genetic, biochemical and environmental signals (Müller and Schmidt, 2004; Salazar-Henao et al., 2016). This process is best understood in *Arabidopsis thaliana*, in which root hairs elongate from longitudinal hair cell files (trichoblasts) that alternate with non-hair cells (atrichoblasts) around the diameter of the primary root (Duckett et al., 1994). Root hairs initiate in a distinct longitudinal pattern, growing only in the maturation zone, which begins approximately 1.5 mm from the root tip (Verbelen et al., 2006). Root hairs function in nutrient and water uptake, and precise regulation of their formation is linked to nutrient and moisture availability (Giehl and von Wirén, 2014; Müller and Schmidt, 2004).

Genetic mechanisms establishing trichoblast and atrichoblast cell fate were elucidated in *Arabidopsis* mutants with altered root hair number (Salazar-Henao et al., 2016), revealing transcription factors (TFs) that define cell fate (Masucci et al., 1996; Wada et al., 1997; Lee and Schiefelbein, 1999; Walker et al., 1999; Bernhardt et al., 2003; Lin et al., 2015). Transcriptomic studies have revealed features of the gene regulatory networks that control root hair development (Bruex et al., 2012; Feng et al., 2017; Kwasniewski et al., 2013, 2016).

Department of Biology and Centers for Molecular Signaling and Redox Biology and Medicine, Wake Forest University, Winston-Salem, NC 27109, USA.

*Author for correspondence (muday@wfu.edu)

S.R.G., 0000-0002-3395-683X; G.K.M., 0000-0002-0377-4517

Mutant screens also identified the *rhd2* mutant for its impaired root hair elongation (Schiefelbein and Somerville, 1990). This mutation maps to the *RESPIRATORY BURST OXIDASE HOMOLOGUE C* (*RBOHC*) locus (Foreman et al., 2003). RBOH enzymes are signaling-regulated and membrane-localized enzymes that produce superoxide, which can be converted to hydrogen peroxide (H_2O_2) to control development and stress responses (Chapman et al., 2019). Localization of RBOHC at the root hair tip creates a tip-focused ROS gradient (Foreman et al., 2003) in elongating root hairs (Jones et al., 2007), which drives a Ca^{2+} gradient, exocytosis and subsequent elongation (Foreman et al., 2003).

ROS act as signaling molecules at low levels but can accumulate in response to stress and cause cellular damage and cell death at high levels (Chapman et al., 2019). Plants maintain ROS homeostasis through enzymatic and non-enzymatic ROS-scavenging mechanisms that are conserved across most eukaryotes, but also produce specialized metabolites as a unique approach to the maintenance of ROS homeostasis (Agati et al., 2012; Chapman et al., 2019). One such class of specialized metabolites are flavonoids, which include flavonols and anthocyanins. The protective function of anthocyanin antioxidants have been studied in shoot tissues (Agati and Tattini, 2010; Agati et al., 2012; Kim et al., 2017; Nakabayashi et al., 2014b; Teng et al., 2005; Watanabe et al., 2018). Roots produce flavonols, but not anthocyanins, due to a lack of synthesis of enzymes that synthesize anthocyanins (Lewis et al., 2011; Maloney et al., 2014). Plants with mutations in flavonol synthesis have tissue-specific increases in ROS accumulation that affect downstream ROS-dependent signaling, including guard cell closure (Watkins et al., 2014, 2017), pollen tube elongation in ambient and high temperatures (Muhlemann et al., 2018), and root hair development (Maloney et al., 2014). The *anthocyanin reduced* (*are*) tomato mutant has reduced flavonol levels in roots, increased root hair numbers, and elevated epidermal and root hair ROS accumulation (Maloney et al., 2014). Flavonols have also been implicated as negative regulators of auxin transport (Gayomba et al., 2016). Mutants with impaired flavonol synthesis have elevated auxin transport (Brown et al., 2001; Buer and Muday, 2004; Lewis et al., 2007; Maloney et al., 2014; Murphy et al., 2000; Peer et al., 2004) and these differences have been tied to root branching (Brown et al., 2001), leaf morphology (Ringli et al., 2008) and gravitropism (Lewis et al., 2007). Flavonol levels also control the oxidation of an auxin indole-3-acetic acid (IAA) (Peer et al., 2013), and elevated auxin levels increase the ROS status of cells (Jiang et al., 2003; Joo et al., 2001). Mutants with defects in ROS homeostasis revealed that auxin transport is also regulated by ROS levels (Fernández-Marcos et al., 2013). These studies indicate complex interplay between flavonols, ROS and auxin transport.

We have uncovered a role for flavonol antioxidants in modulating root hair initiation in *Arabidopsis*. ROS-specific fluorescent dyes reveal elevated ROS levels in the root epidermis of mutants defective in flavonol synthesis. Flavonol accumulation and

expression of green fluorescent protein (GFP) fusions to flavonol biosynthetic enzymes are at low levels in the epidermis, allowing ROS to promote root hair formation. The flavonoid-deficient mutant *transparent testa 4* (*tt4*) has increased root hair number and ROS levels in trichoblast cells relative to the wild type. The root hair phenotypes of *tt4* can be reversed by genetic or chemical complementation and by altering ROS status with antioxidants, supporting the function of flavonols in modulating ROS levels that drive root hair formation. Auxin treatment of *tt4* and the RBOHC-deficient mutant *rhd2-6* suggests that ROS and auxin work together to enhance root hair initiation. This study highlights the role of ROS signaling in root hair development and provides insight into the spatial control of flavonol synthesis and their role in modulating ROS homeostasis and ROS-dependent development.

RESULTS

Flavonols and reactive oxygen species have opposite localization patterns in the root epidermis

The distribution of ROS accumulation in wild-type (Col-0) *Arabidopsis* roots was examined using a general ROS fluorescent sensor, 5-(and 6)-chloromethyl-2′,7′-dichlorodihydrofluorescein diacetate (CM-H$_2$DCFDA), to investigate whether ROS localizes to areas of root hair development. After uptake, endogenous esterases cleave the acetate group of CM-H$_2$DCFDA and the product, 7′-dichlorofluorescein (DCF), fluoresces upon ROS oxidation. The brightest DCF signal was observed within epidermal cells in the maturation zone and root hairs (Fig. 1A-D), with the apical 500 µm at the root tip having lower DCF signal (Fig. 1C). Fig. 1C also indicates how we divided the root into two developmental zones for analyses. Zone 1 encompasses a 1500 µm region from the tip to the beginning of that maturation zone, including the area of root hair initiation. Zone 2 spans the next 1000 µm of the root and is within the maturation zone, where previously formed root hairs elongate.

Elevated ROS in root hairs and trichoblast cells compared with atrichoblasts is reminiscent of a prior report describing a similar localization for the RBOHC enzyme and a root elongation phenotype in *rhd2-6*, an *rbohc* mutant (Foreman et al., 2003). We examined *rhd2-6* and found a reduced tip-focused DCF gradient in the root apex and in root hairs (Fig. 1E,F) compared with Col-0, similar to that reported by Foreman et al. (2003). In contrast, the *tt4-11* mutant, which does not produce flavonol antioxidants, had an accentuated ROS gradient in the root tip (Fig. 1E,F), suggesting that flavonols might function to reduce ROS levels in the root epidermis and root hairs.

If flavonol antioxidant activity reduces ROS levels, their accumulation should be higher in regions with lower DCF fluorescence. We analyzed the localization patterns of flavonols in Col-0 roots using the probe 2-aminoethyl diphenylboric acid (DPBA) (Sheahan and Rechnitz, 1992). *In vivo* fluorescence differs between kaempferol-DPBA (green shifted) and quercetin-DPBA (yellow shifted), allowing distinct visualization of these two flavonols (and the glycosylated conjugates) by laser scanning confocal microscopy (LSCM) (Lewis et al., 2011). Kaempferol-DPBA and quercetin-DPBA fluorescence was visualized by LSCM and was highest in the elongation zone in Col-0 roots (Fig. 2A). Here, ROS are held at lower levels, as judged by lower DCF fluorescence in the same position (Fig. 2B). The DPBA signal extended into the more distal regions from the root tip, with decreasing intensity at the maturation zone, suggesting lower flavonol levels in this region. Accordingly, DCF fluorescence was higher in the maturation zone compared with the root tip (Fig. 1A, Fig. 2B,D).

To better define flavonol localization and accumulation, we examined optical sections of the whole root (Fig. 2C) or root tip and maturation zone (Fig. 2E-N). Quercetin and kaempferol levels were highest in a region 200 µm from the root tip (Fig. 2J-L). Quercetin accumulated in high abundance in the transition zone (Fig. 2K,M), whereas the strongest kaempferol signal was detected in the vasculature (Fig. 2C,L,N). These flavonols also show different subcellular locations, with only quercetin accumulating in the nucleus of unelongated cells (Fig. 2K) where it colocalized with Hoechst stain (Fig. S1), consistent with prior reports of nuclear localization of pathway enzymes and DPBA colocalization with DAPI or Hoechst stain (Saslowsky et al., 2005; Watkins et al., 2014).

In the maturation zone, kaempferol fluorescence was lower compared with quercetin (Fig. 2F-I) and both flavonols were
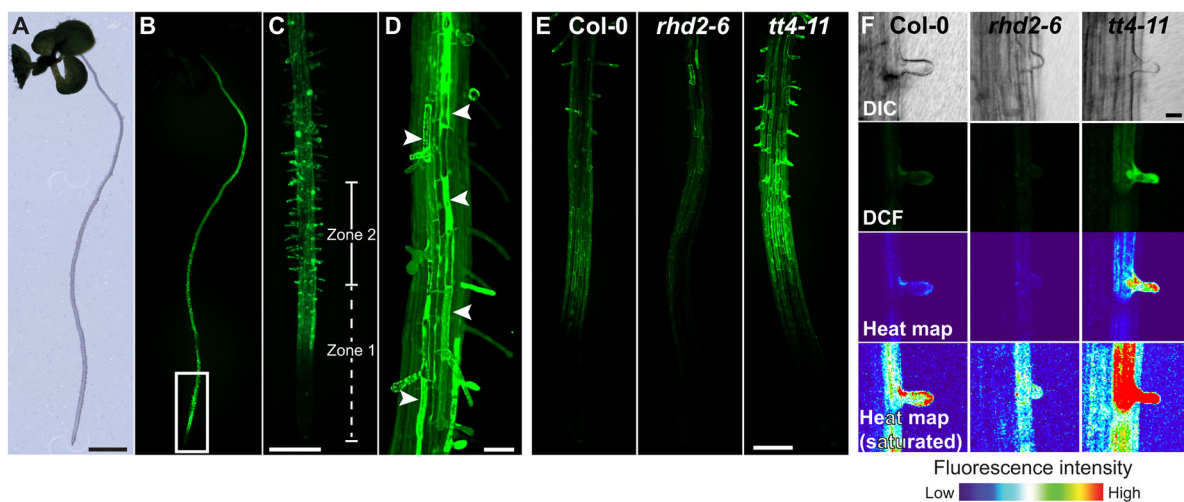

Fig. 1. ROS accumulation in root hair and trichoblast cell files are modulated by RBOHC and flavonols. (A-D) Stereomicroscope images of Col-0 stained with CM-H$_2$DCFDA in bright field (A) and DCF fluorescence (B). (C) Magnification of the white box in B shows DCF accumulation in the root apex. Root hair number was quantified in zone 1 and/or zone 2. (D) DCF accumulation in root hairs and epidermal tissue in saturated images. Arrowheads indicate greater fluorescence in trichoblasts. (E) DCF fluorescence in LSCM images of Col-0, *rhd2-6* and *tt4-11* seedlings. (F) ROS levels in elongating root hairs of the indicated genotypes are presented as DIC, DCF, and heat maps of LSCM DCF images. Scale bars: 2 mm (A,B); 500 µm (C); 100 µm (D); 200 µm (E); 20 µm (F).
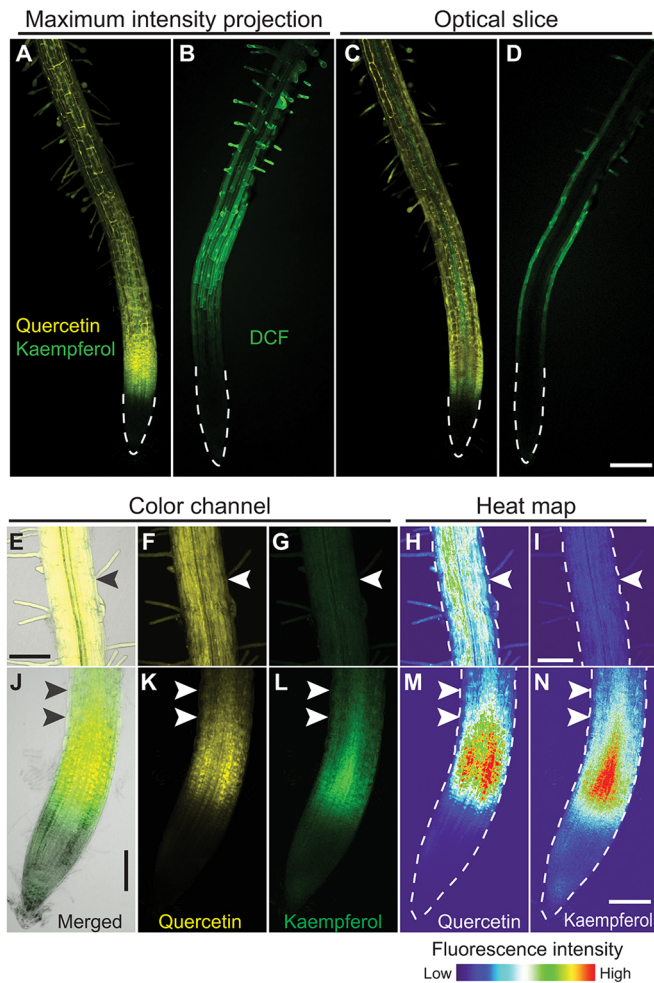
Fig. 2. Flavonol levels are low in the epidermis where ROS accumulates.
(A,C) Col-0 roots stained with DPBA allows visualization of quercetin (yellow) and kaempferol (green) flavonols. (B,D) ROS accumulation was reported by DCF fluorescence in maximum intensity projections of z-stack images (A,B) or optical sections of the center of the root (C,D). Dashed lines indicate the root tip. Scale bar: 200 μm. (E-N) Optical sections of quercetin and kaempferol accumulation in the root tip and maturation zone under higher magnification. Color channels show merged images of quercetin, kaempferol and DIC (E,J), quercetin (F,K) or kaempferol (G,L). Arrowheads indicate the epidermis. Heat maps of color images (H,I,M,N) indicate the scale of fluorescence intensity. Arrowheads and dashed lines indicate the epidermal layer. Scale bars: 100 μm. Representative images of three independent LSCM experiments (n=6 seedlings/experiment) are shown.

Fig. 3. CHS-GFP and FLS1-GFP fluorescence is low in the root epidermis.
(A-L) LSCM mages of CHS-GFP and FLS1-GFP fluorescence (green) and cell walls stained with propidium iodide (PI, magenta) with epidermal tissues indicated with dashed lines and arrowheads at the apex (A-D) and mature region (E-L) of roots. Scale bars: 100 μm. Panels A-F, I and J are optical slices, whereas G,H and K,L are maximum projection images. Representative images of three independent experiments (n=6 seedlings/experiment) are shown.

observed in different cell layers in which DCF fluorescence accumulates (Fig. 2C). DCF fluorescence accumulates in the epidermis (Fig. 2D), whereas quercetin and kaempferol levels were low in this layer (Fig. 2E-H,M,N). The difference in DPBA fluorescence between epidermal and inner tissues is more evident when fluorescence intensities are represented as a heat map (Fig. 2H,I,M,N). Low levels of flavonol antioxidants in the epidermis and root hairs are consistent with the higher ROS accumulation observed in these tissues (Fig. 2B,D).

Chalcone synthase and flavonol synthase protein levels are low in the epidermis
We asked whether the low flavonol accumulation in the epidermis was due to decreased flavonol biosynthesis. The first committed step of flavonoid synthesis is catalyzed by chalcone synthase (CHS)
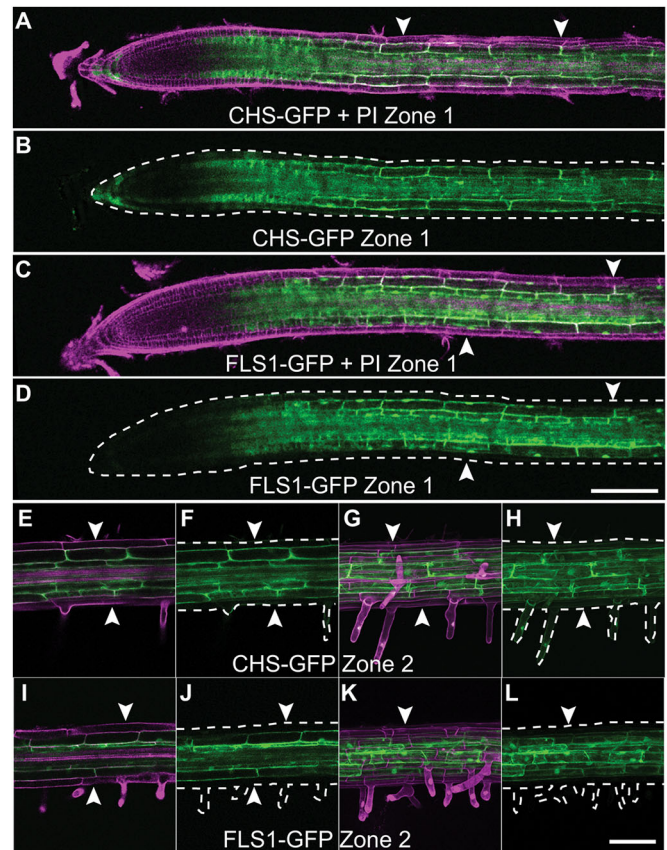
(Gayomba et al., 2016), whereas the majority of flavonols are converted from dihydroflavonol compounds by flavonol synthase 1 (FLS1) (Forkmann et al., 1986; Holton et al., 1993). Localization of CHS and FLS1 was examined using translational fusions to GFP (Lewis et al., 2011; Kuhn et al., 2011) under the control of their native promoters (Fig. 3).

Optical sectioning by LSCM showed that *CHSpro::CHS-GFP* (CHS-GFP) and *FLS1pro::FLS1-GFP* (FLS1-GFP) fluorescence in zone 1 accumulated in high abundance in the inner tissues and was substantially lower in the epidermal cells (Fig. 3A-D). Imaging seedlings using increased laser power revealed CHS-GFP and FLS1-GFP signals in the epidermis of both transgenic lines (Fig. S2), confirming that these enzymes were present in the epidermis, but at markedly lower concentrations compared with inner tissues. In the mature region of the root, low fluorescence was again observed in the epidermis for both CHS- and FLS1-GFP seedlings (Fig. 3E,F,I,J). When we analyzed fluorescence as a maximum intensity projection of z-stack images, root hairs had low or nondetectable fluorescence of CHS-GFP or FLS1-GFP, respectively (Fig. 3G-L). However, under increased laser power, fluorescence signal was detected in root hairs of both transgenic lines (Fig. S2). These results demonstrate spatial regulation of flavonol accumulation through tissue-specific synthesis of biosynthetic enzymes.

Mutants with reduced flavonol levels have increased root hair number that is reversed by genetic and chemical complementation

We employed a genetic approach to test whether flavonol antioxidants modulate ROS to control root hair formation using mutants that do not produce flavonols. The *tt4-2* and *tt4-11* mutants contain mutations in the single gene encoding CHS in *Arabidopsis* (Koornneef, 1990; Shirley et al., 1995) and do not produce flavonoids (Fig. 4). The FLS1 isoenzyme synthesizes the majority of flavonols *in vivo* (Owens et al., 2008; Preuss et al., 2009) and the *fls1-3* mutant contains a premature stop codon in the first exon of *FLS1* (Kuhn et al., 2011). We verified that these mutants produce no or low flavonols in roots (Fig. 4) and shoots (Fig. S3) using liquid chromatography-mass spectroscopy. Root levels of naringenin, the flavonol precursor, and the three flavonols kaempferol, quercetin and isorhamnetin were overlaid on the biochemical pathway shown in Fig. 4 to show accumulation differences as a result of defects in specific enzymes.

The root hair pattern in the *tt4* and *fls1* mutants in zone 1, where root hairs initiate and elongate (Verbelen et al., 2006), is shown in Fig. 5A. When root hair number is quantified in this defined region

Fig. 4. Mutants in genes encoding enzymes of the flavonoid biosynthetic pathway in *Arabidopsis* show altered metabolite concentrations in roots. Enzymes are next to arrows, with corresponding mutant names in parentheses. Mutant names in bold are used in this study. Chemical structures for specific flavonols are shown in the upper right. The abundance of the flavonol precursor naringenin, and flavonols kaempferol, quercetin and isorhamnetin, were quantified in root extracts from seedlings of the indicated genotypes. Data are mean±s.e.m. from four independent experiments reported as μmol/mg fresh weight. Bars with different letters indicate statistically significant differences determined by one-way ANOVA. ND (not detected) indicates flavonoid levels below the limit of detection or at background levels.

of the root, both *tt4* alleles and the *fls1-3* mutant exhibited statistically significant increases in root hair number compared with Col-0 in both zone 1 (Fig. 5B) and zone 2, which is further back from the root tip (Fig. 5C,D). The effect of this mutation on root hair number in a defined region of the root could be because of differences in root hair initiation or because of shorter trichoblast cells. We measured the distance of trichoblast cells in Col-0 and *tt4* alleles and found no differences in zone 1, although the length of these cells in zone 2 was reduced in the *tt4-11* allele compared with Col-0, whereas *tt4-2* was at an intermediate length (Fig. 5F). The small but significant differences in length of the epidermal cells in zone 2 cannot account for the increased number of root hairs; over the length of zone 2 the small difference in length would only account for two additional epidermal cells, but the difference in number of root hairs (six in Col-0 and 15 in *tt4-11*) is greater than would be predicted by this difference in length.

To better illustrate the developmental difference in root hair formation, a higher resolution image of zone 2 of Col-0 and the two *tt4* alleles is shown in Fig. 5G. A magenta line is used to indicate a single trichoblast cell file. This image shows that the frequency of trichoblast cells that form root hairs is much lower in Col-0 than in the two *tt4* alleles, consistent with flavonol inhibition of root hair initiation in wild type and release of this repression in the absence of flavonols in *tt4*.

To verify that the root hair phenotype was due to altered flavonol synthesis, root hair number was examined in a *tt4-11* mutant complemented with *CHS-GFP*, which reduced root hair number relative to untransformed *tt4-11* mutants (Fig. 5A,B). We also chemically complemented both *tt4* mutant alleles with naringenin treatment. Naringenin is produced downstream of CHS (Fig. 4) and restores flavonol production to wild-type levels in the *tt4-2* mutant (Buer et al., 2007). Treatment of 5-day-old Col-0 and *tt4* mutants for 24 h was sufficient to increase flavonol synthesis to wild-type levels (Fig. S4) and to restore wild-type root hair formation in both zone 1 and zone 2 (Fig. 5C-E). In contrast, naringenin treatment did not affect root hair number in Col-0 in either zone at the concentrations tested (Fig. 5C-E), consistent with no additional flavonol synthesis even with excess substrate in wild type.

Mutants with reduced flavonol levels have elevated levels of hydrogen peroxide in trichoblasts

To determine whether there is higher ROS level in *tt4* mutants because of the absence of flavonol antioxidant activity, we examined Col-0 and *tt4* seedlings stained with ROS-sensitive dyes using LSCM. A 4 min stain with CM-H$_2$DCFDA showed a brighter DCF signal in the epidermis than in internal tissues in all three genotypes, with more intense signal in the *tt4* alleles (Fig. 6A). When DCF fluorescence intensity was presented as a plot profile along the epidermis in zone 1, both *tt4* alleles had significantly higher fluorescence compared with Col-0 (Fig. 6B). We also quantified the total DCF signal in the epidermis and found statistically significant increases in both *tt4* alleles when the signal of the entire root tip was quantified (Fig. S5A).

To verify that differences in DCF fluorescence between Col-0 and *tt4* mutants were not due to differences in dye uptake or esterase activity, we stained seedlings with fluorescein diacetate (FDA) (Fig. S5). FDA is structurally similar to CM-H$_2$DCFDA, but its fluorescence depends only on esterase activity, not ROS (Rotman and Papermaster, 1966). Similar FDA fluorescence was observed between Col-0 and *tt4-11*, with a slightly lower signal in *tt4-2* (Fig. S5B,C) and yielded distinct plot profile patterns compared with DCF (Fig. S5D). These controls are consistent with increased DCF
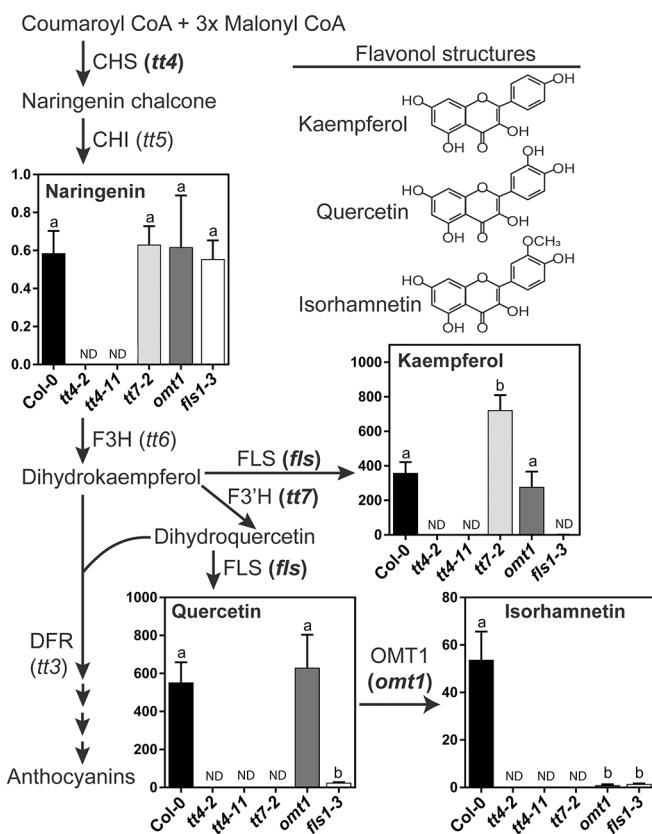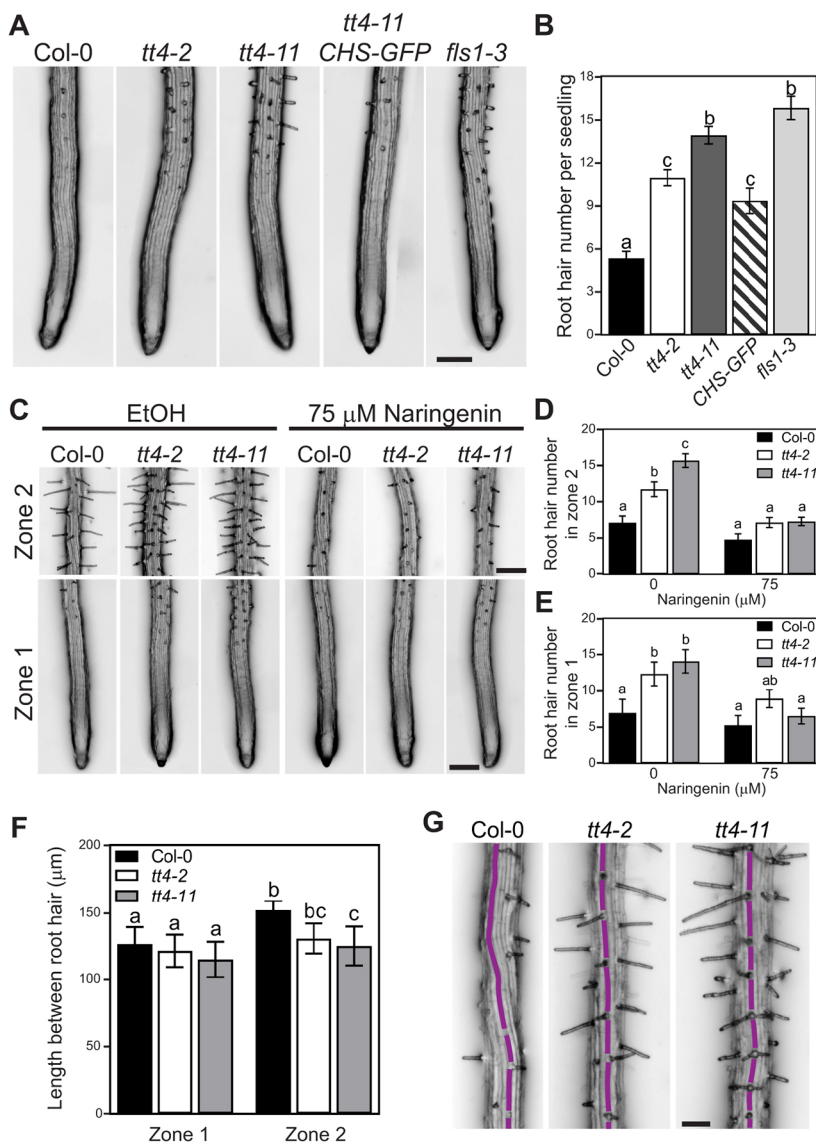
Fig. 5. Absence of flavonols increases root hair number and is reversed by naringenin treatment. (A) Representative images of root hair number in Col-0, *tt4-2*, *tt4-11* and *tt4-11* complemented with the *CHSpro::CHS-GFP* transgene, and *fls1-3*. Scale bar: 200 μm. (B) Root hair quantification of genotypes in A. Data are mean±s.e.m. of three independent experiments (*n*=20-25 seedlings/ experiment). (C) Representative images of Col-0, *tt4-2* and *tt4-11* seedlings, after mock or naringenin treatment. EtOH, ethanol. Scale bars: 200 μm. (D) Root hair quantification in zone 2 and (E) zone 1 24 h after mock or naringenin treatment. Data are mean±s.e.m. of four independent experiments (*n*=5-17 seedlings/experiment). (F) The length of trichoblast cells in untreated Col-0 and *tt4* alleles were measured. Data are mean±s.e.m. of lengths between a minimum of three root hairs in two separate trichoblast files from three independent experiments (*n*=3-14 seedlings/ genotype for each experiment). Columns with different letters in B,D,E,F, indicate statistically significant values, whereas columns with the same letters are not statistically different according to one-way ANOVA (B,F) or two-way ANOVA (D,E). (G) Images of zone 2 in Col-0, *tt4-2* and *tt4-11*, with the length of a single trichoblast cell highlighted in magenta to clarify that greater frequency of root hair formation occurs in the *tt4* alleles than Col-0, which has many more trichoblasts that do not form root hair. Scale bar: 100 μm.

fluorescence in the *tt4* mutants being linked to elevated ROS levels in the absence of flavonols, not increased esterase activity or dye uptake.

To determine which ROS is elevated in *tt4* roots, we measured H_2O_2 accumulation using the H_2O_2-specific dye Peroxy Orange1 (PO1) (Dickinson et al., 2010; Winterbourn, 2014). Plot profiles of epidermal PO1 fluorescence revealed slightly higher fluorescence intensity in *tt4-11*, with similar longitudinal patterns of fluorescence in all genotypes (Fig. S6A,B). When average fluorescence intensity per seedling using optical slices through the center of the root was quantified, PO1 fluorescence was slightly, but significantly, higher in the epidermis of the *tt4-11* mutant compared with Col-0, whereas fluorescence in the *tt4-2* allele was at an intermediate level (Fig. S6C).

However, when PO1 fluorescence was analyzed in trichoblast and atrichoblast cells at the surface of the root, we found more dramatic differences between Col-0 and the *tt4* mutant alleles (Fig. 6C,D). We quantified fluorescence intensity across five cell files in zone 2 and found that *tt4* seedlings, but not Col-0, had significantly higher fluorescence in trichoblast cells compared with atrichoblast cells, and that levels were significantly higher in trichoblasts of *tt4* than in Col-0 (Fig. 6C,D).

We also investigated whether naringenin treatment, which reversed the root hair phenotype of *tt4* mutants, would also

reduce PO1 fluorescence in *tt4* to wild-type levels. Naringenin treatment did not alter PO1 fluorescence in Col-0 compared with mock-treated controls (Fig. 6C,D). In contrast, PO1 fluorescence intensity was reduced in trichoblast cells of naringenin-treated *tt4* mutants.

We tested whether increased ROS-dependent fluorescence in trichoblasts of *tt4* roots was due to higher dye uptake, facilitated by increased root hair number. We stained Col-0, *tt4-2* and *tt4-11* with CM-H_2DCFDA or FDA and compared fluorescence patterns of epidermal cell files. Like PO1, DCF fluorescence was increased in trichoblast cells of *tt4* alleles compared with Col-0 (Fig. S7), whereas FDA-stained seedlings showed similar fluorescence across cell files.

Elevated hydrogen peroxide drives root hair formation in *tt4*

To investigate whether elevated H_2O_2 in trichoblasts drives root hair formation, we treated 5-day-old Col-0, *tt4-2* and *tt4-11* seedlings with an H_2O_2 scavenger, potassium iodide (KI) (Dunand et al., 2007; Liebhafsky, 1934), and quantified root hair number in zone 1 after 24 h. Under control conditions, *tt4* seedlings had higher root hair numbers than Col-0, and KI treatment reduced *tt4* root hair number to wild-type levels (Fig. 7A,B), but did not affect root hair number in
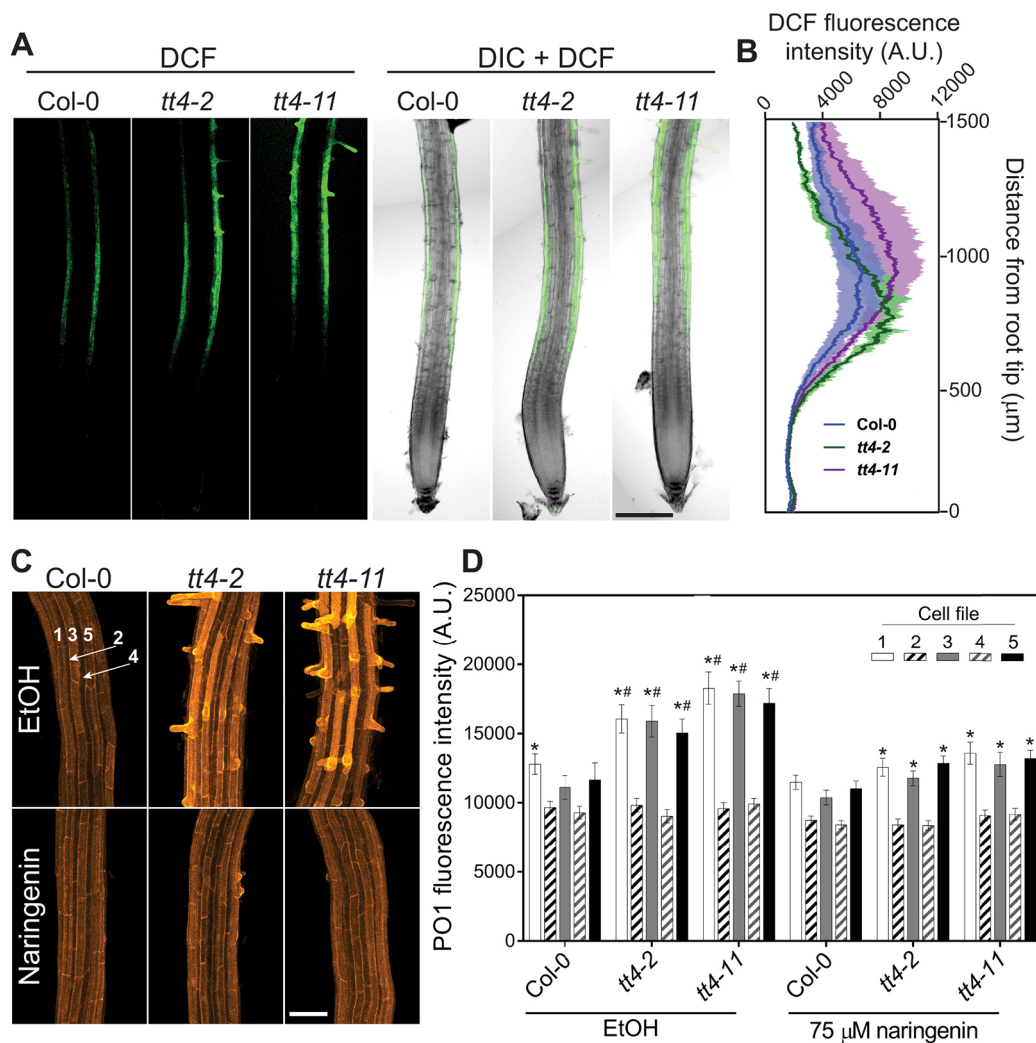
5

Fig. 6. Epidermal ROS is increased in the absence of flavonols in the *tt4* mutants. (A) Representative epidermal DCF fluorescence of Col-0, *tt4-2* and *tt4-11* seedlings (left panels) and merged DCF and DIC images (right panels). Images are scaled to correspond to the *y*-axis of the plot profile in D. Scale bar: 200 μm. (B) Plot profiles of epidermal DCF fluorescence in Col-0, *tt4-2* and *tt4-11* seedlings. Data are mean±s.e.m. of three independent experiments (*n*=10-15 seedlings/experiment). (C) Representative images of PO1 fluorescence in zone 2 of Col-0, *tt4-2* and *tt4-11*. Trichoblast cell files are labeled 1, 3 and 5; atrichoblast cells are 2 and 4. EtOH, ethanol. Scale bar: 50 μm. (D) Quantification of epidermal PO1 fluorescence in zone 2 of Col-0, *tt4-2* and *tt4-11* seedlings 24 h after mock or naringenin treatment. Data are mean±s.e.m. of three independent experiments (*n*=5-8 seedlings/genotype per treatment for each experiment). Asterisks indicate statistically significant differences between trichoblast and atrichoblast cell files within a group. # indicates statistically significant differences in fluorescence intensity in trichoblast cell files in *tt4* mutants compared with Col-0. Fluorescence in atrichoblast cell files were not significantly different between treatments or genotypes. Statistics were determined by two-way ANOVA.

Col-0. PO1 staining verified that KI treatment reduced H_2O_2 levels in trichoblasts of the *tt4* mutants to wild-type levels and eliminated the difference between trichoblasts and atrichoblasts in *tt4* (Fig. 7C; Fig. S8). These images also show that trichoblasts in the *tt4* mutants accumulated H_2O_2 prior to root hair elongation (Fig. 7), consistent with H_2O_2 being the ROS molecule driving root hair initiation.

The *rhd2-6* mutant does not have elevated H_2O_2 in trichoblasts and has reduced auxin response

Root hair elongation has been linked to the localization and activity of the RBOHC enzyme (Foreman et al., 2003; Carol et al., 2005; Takeda et al., 2008; Jones et al., 2007). *RBOHC-GFP* and *RBOHC-GUS* fusions have signal in the root epidermis (Lee et al., 2013; Takeda et al., 2008) and *RBOHC-GFP* and *RBOHC* transcripts preferentially localize in trichoblasts in the elongation and maturation zones (Brady et al., 2007; Takeda et al., 2008). The trichoblast expression pattern of *RBOHC* matches the increased

ROS signal in trichoblasts of the *tt4* mutants, whereas the alternating DCF accumulation profile between trichoblast and atrichoblast cell files and tip-focused DCF gradient in root hairs are lost in *rhd2-6* (Fig. 1). The pattern of elevated PO1 in trichoblasts relative to atrichoblasts was also lost in *rhd2-6*, with all cell files in the mutant having equivalent levels of PO1, which represents a reduced gradient compared with Col-0 (Fig. S9).

We investigated whether PO1 accumulation in trichoblasts and root hair formation was increased by treating seedlings with the auxin indole-3-acetic acid (IAA), which is a positive regulator of root hair formation (Salazar-Henao et al., 2016). Agar droplets containing 0.1 μM IAA or ethanol (mock treatment) were applied to the root tips of Col-0, *tt4-11* or *rhd2-6* to increase shootward transport of auxin into the region where root hairs initiate. If IAA-induced root hair formation requires RBOHC, we would expect *rhd2-6* mutants to show no increases in ROS or root hair number after IAA treatment. When mock-treated seedlings were stained
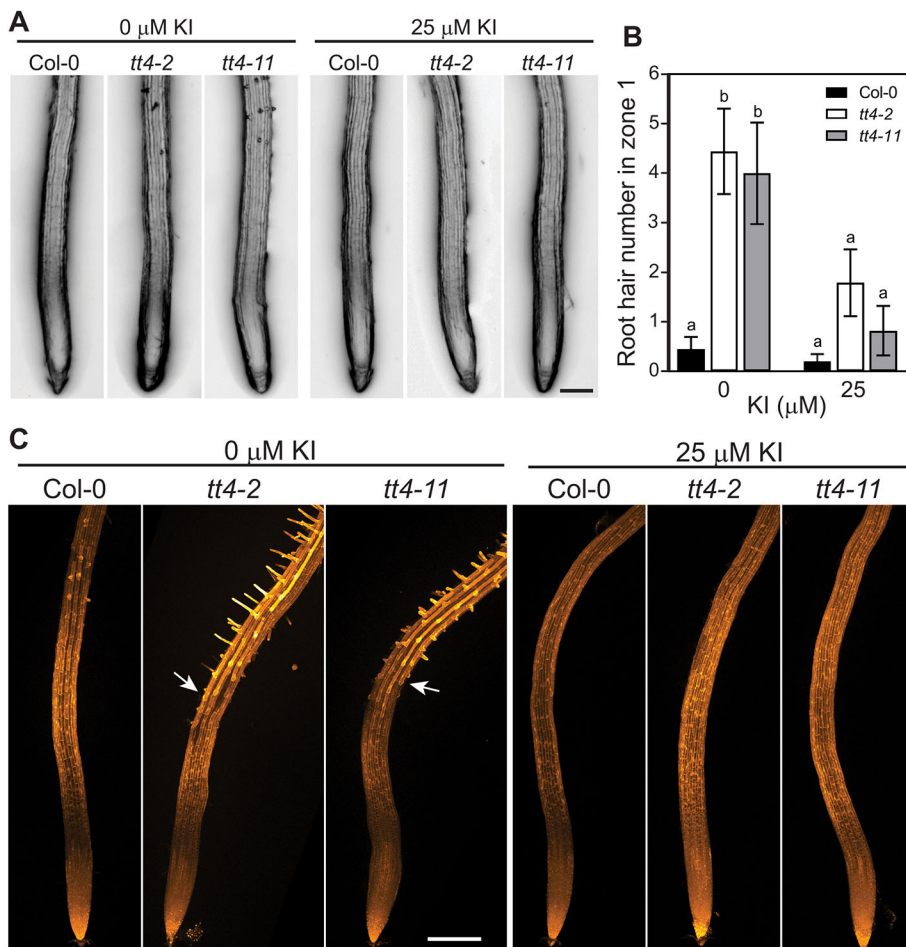
Fig. 7. H$_2$O$_2$ is a positive regulator of root hair number. (A) Representative images of root hairs in zone 1 of Col-0, *tt4-2* and *tt4-11* seedlings, treated with or without 25 µM KI. Scale bar: 200 µm. (B) Root hair quantification in zone 1 of the genotypes indicated in A. Data are mean±s.e.m. of three independent experiments (*n*=5-10 seedlings/experiment). Columns with different letters indicate statistically significant differences determined by two-way ANOVA. (C) Representative epidermal PO1 fluorescence patterns in Col-0, *tt4-2* and *tt4-11* seedlings, with or without KI. Arrows indicate increases in fluorescence in trichoblast cells prior to root hair elongation. Scale bar: 200 µm.

with PO1, the pattern of PO1 elevation in the trichoblast cells was evident in Col and *tt4-11* and dampened in the *rhd2-6* mutant (Fig. 8A), with no detectable differences between trichoblast and atrichoblast cells of *rhd2-6* (Fig. S9). In contrast, IAA treatment increased PO1 fluorescence in trichoblasts of Col-0 and *tt4-11* seedlings, but not in *rhd2-6* mutants (Fig. 8B).

When newly formed root hairs were quantified, root hair numbers remained elevated in the mock-treated *tt4-11* mutant compared with Col-0 and *rhd2-6* (Fig. 8C). IAA treatment also increased root hair number in the *tt4-11* mutant, whereas IAA-treated Col-0 had root hair numbers that were not statistically different from mock-treated Col-0 (Fig. 8C). This finding is consistent with elevated auxin transport in *tt4-11* leading to increased root hair formation. In the *rhd2-6* mutant, the number of root hairs did not change with IAA treatment (Fig. 8C). These results confirm that IAA increases ROS and that this increase in trichoblast cells depend on RBOHC. Additionally, the lack of root hair induction in *rhd2-6* when treated with IAA suggests that ROS and auxin work in concert to initiate root hairs.

Higher levels of ROS and auxin transport act synergistically in root hair formation in the *tt4* mutant

Auxin transport through epidermal cells promotes root hair development (Jones et al., 2002; Dindas et al., 2018) and auxin transport from the root tip is enhanced in *tt4* mutants owing to the absence of flavonols, which negatively regulate shootward auxin transport (Buer and Muday, 2004; Gayomba et al., 2016; Lewis et al., 2007). We examined the effect of IAA on newly formed root hairs by comparing images taken at the time of treatment with those

taken 4 h later (Fig. S10) and found that IAA treatment of Col-0 and *tt4-11* increased root hair number (Fig. 8). If auxin transport is enhanced in the *tt4-11* mutant, root hairs should form further from the root tip in *tt4-11* compared with Col-0. When the position and number of newly formed root hairs were plotted along the root, mock-treated *tt4-11* seedlings formed root hairs further from the tip than did Col-0 (Fig. 9A,B), consistent with the lack of an endogenous auxin transport inhibitor. Treatment with IAA reduced cell elongation in roots, shifting the position of newly formed root hairs closer to the root tip of IAA-treated plants (Fig. 9B). Nevertheless, root hairs formed in the *tt4-11* mutant were further from the root tip compared with Col-0 (Fig. 9A,B). These results suggest that increased auxin transport, as well as altered ROS status, contributes to enhanced root hair number in the *tt4* mutants.

Quercetin is the active flavonol in regulating root hair development

The absence of flavonols in the *tt4* alleles and reduction of flavonols in *fls1-3* suggests a role for flavonols in controlling root hair development but does not reveal whether one specific flavonol is responsible for this effect. We investigated which flavonol regulated root hair initiation using the *tt7-2* and *omt1* mutants, which contain T-DNA insertions in the gene encoding flavonoid 3′-hydroxylase, *F3′H* (Lewis et al., 2011), and O-methyltransferase 1, encoded by *OMT1* (Tohge et al., 2007), respectively. The F3′H enzyme converts dihydrokaempferol to dihydroquercetin, a precursor for quercetin and isorhamnetin (Schoenbohm et al., 2000). OMT1 methylates quercetin to produce isorhamnetin (Muzac et al., 2000;
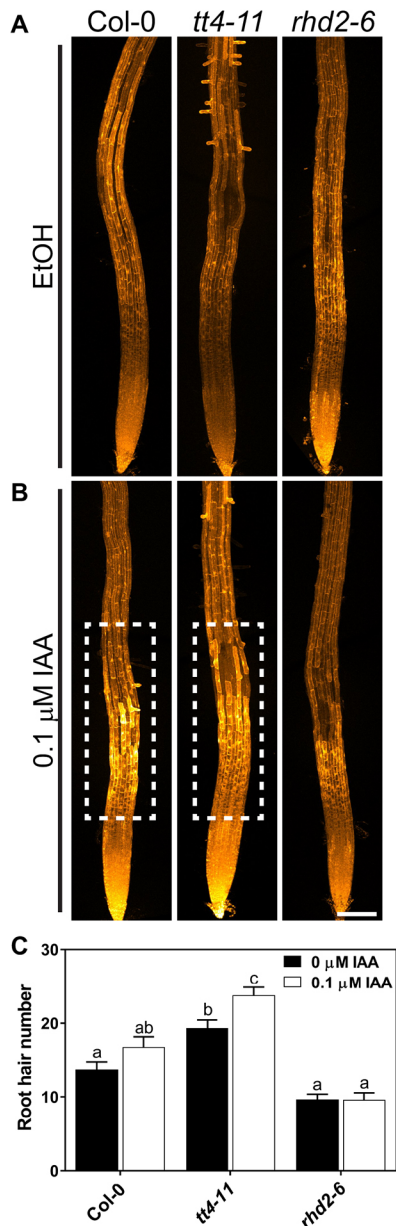
Fig. 8. IAA increases H$_2$O$_2$ through RBOHC. (A,B) Col-0, *tt4-11* and *rhd2-6* seedlings, stained with PO1 after 4 h of (A) ethanol (EtOH) or (B) 0.1 µM IAA application to the root tip. The dashed boxes show increased PO1 signal in Col-0 and *tt4-11* after IAA treatment, which is absent in *rhd2-6*. Scale bar: 200 µm. (C) Root hair number formed after 4 h of the indicated treatments. Data are mean±s.e.m. of three independent experiments (*n*=6-12 seedlings/ genotype per experiment). Columns with different letters indicate statistically significant differences determined by two-way ANOVA.

Tohge et al., 2007). Thus, the *tt7* mutant produces only kaempferol, whereas the *omt1* mutant synthesizes kaempferol and quercetin in root (Fig. 4) and shoot (Fig. S3) tissues.

tt4-2 and *tt7-2* mutants had increased root hair numbers compared with Col-0 (Fig. 10A,B). The magnitude of induction was similar between *tt4* and *tt7*, suggesting that this phenotype is due to the lack of quercetin. In contrast, root hair numbers in the *omt1* mutant were similar to Col-0 (Fig. 10A,B). These results indicate that quercetin and its glycosylated products are the flavonol antioxidants that control ROS accumulation to modulate root hair development.

DISCUSSION

ROS are important signaling molecules involved in development and stress responses in plants and animals (Mittler et al., 2011; Ray et al., 2012). In plants, antioxidant enzymes and specialized metabolites with antioxidant activity play a key role in allowing productive ROS signaling by preventing ROS from reaching damaging levels (Chapman et al., 2019). The abundance and localization of ROS molecules control *Arabidopsis* root development (Dunand et al., 2007; Foreman et al., 2003; Orman-Ligeza et al., 2016; Tsukagoshi et al., 2010). The link between root hair elongation and ROS has been clearly established (Carol et al., 2005; Foreman et al., 2003; Jones et al., 2007; Takeda et al., 2008): hydroxyl radicals accumulate at the tip of root hairs to facilitate formation of a tip-focused Ca^{2+} gradient, activating downstream processes required for polarized elongation (Foreman et al., 2003; Monshausen et al., 2007). In this study, we examined root hair initiation to determine whether synthesis of flavonol antioxidants defines the location of ROS accumulation in *Arabidopsis* roots and regulates root hair development.

We tested the role of flavonols in root hair formation using mutants with defects in flavonol synthesis. The *tt4-2* and *tt4-11* mutants synthesize no flavonoids, whereas the *fls1-3* mutant has impaired flavonol synthesis but produces all other pathway intermediates. Similar increases in root hair number in the *tt4* alleles and *fls1-3* indicate that flavonols, rather than the intermediate compounds produced between CHS and FLS1, repress root hair number. The increase in root hair numbers in these flavonol-deficient mutants is due to a greater frequency of trichoblast cells forming root hairs as a result of the elevated ROS signal. Consistent with the role of flavonols as repressors of early root hair development, the restoration of CHS function in the *tt4-11* allele, through genetic complementation with CHS-GFP, or chemical complementation with naringenin, reduced root hair number to wild-type levels. Although previous reports did not identify differences in root hair number between *tt4* and wild-type seedlings (Buer and Djordjevic, 2009; Ringli et al., 2008), those studies had different mutant allele backgrounds (Buer and Djordjevic, 2009) and different nutrient (Ringli et al., 2008) and sucrose (Buer and Djordjevic, 2009) concentrations, which would affect the environmentally sensitive levels of ROS and flavonols. Additionally, we grew seedlings at low density to maximize ethylene diffusion and prevent ethylene-induced root hair formation (Feng et al., 2017; Tanimoto et al., 1995), which might mask differences in root hair number between flavonol mutant genotypes, and used new imaging technology that allowed high-resolution images.

We investigated whether all flavonols are required to repress root hair number or if kaempferol, quercetin or isorhamnetin specifically controls this developmental process. Mutation of the F3′H enzyme abolishes quercetin and isorhamnetin production in the *tt7-2* mutant, resulting in higher kaempferol levels in roots than in Col-0 roots. However, the *tt7-2* mutant formed more root hairs, suggesting that the absence of quercetin or isorhamnetin drives this phenotype. The *omt1* mutant produces wild-type levels of quercetin and isorhamnetin, and its root hair phenotype is similar to that of Col-0. Collectively, the root hair phenotypes in *tt4*, *tt7-2* and *omt1* mutants indicate that quercetin and its glycosylated derivatives control early root hair development. Quercetin is a more potent antioxidant than kaempferol and isorhamnetin (Chapman et al., 2019), which suggests that the role of quercetin in root hair formation might be to modulate the abundance of ROS. Three other studies used a similar genetic approach to identify individual flavonols that regulate other developmental processes. Lewis et al. (2011) demonstrated that quercetin regulated root gravitropism.
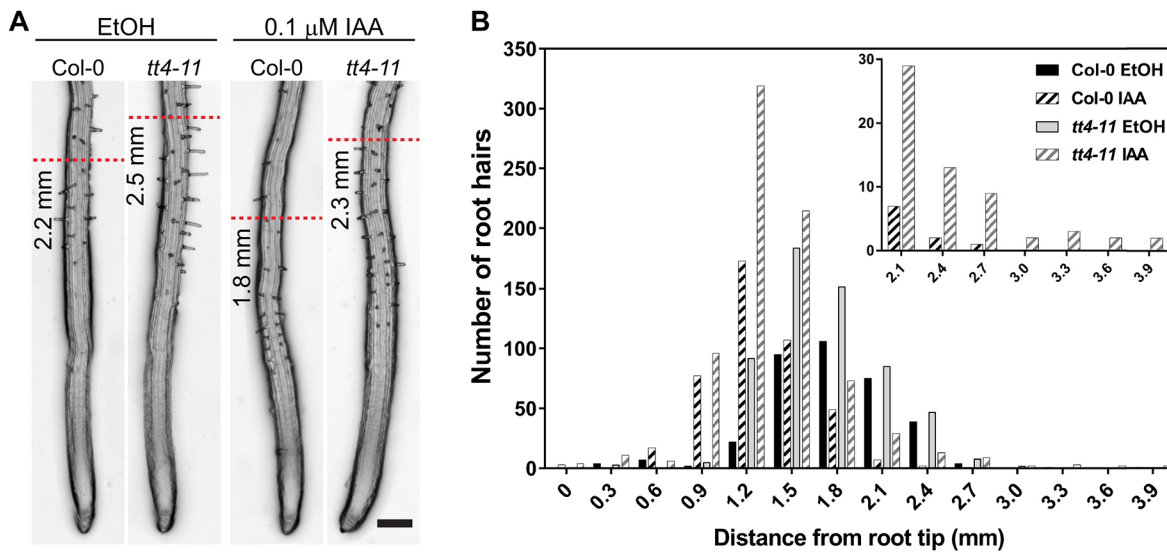
Fig. 9. Increased auxin flux contributes to the root hair phenotype of *tt4* mutants. (A) Representative images of new root hairs formed in Col-0 and *tt4-11* seedlings after 4 h of ethanol (EtOH) or IAA treatment applied to the root tip. The dotted red line indicates the position of the most distal root hair formed after treatment. Scale bar: 200 μm. (B) The position of root hairs formed after treatment were plotted relative to the root tip, which is indicated as 0. The inset shows the region 2-4 mm from the root tip. Root hair positions were generated from three independent experiments (*n*=6-12 seedlings/genotype per treatment for each experiment).

Grunewald et al. (2012) identified a role for quercetin in primary root development, and Ringli et al. (2008) identified a kaempferol derivative that regulated cotyledon morphology. These studies support the model that distinct flavonols have specific roles in plant development.

The location of ROS and flavonols in Col-0 roots suggest that flavonols might regulate root hair formation by controlling ROS homeostasis. Flavonols and their biosynthetic enzymes were at high

Fig. 10. Quercetin is the active flavonol in repressing root hair numbers. (A) Representative images of root hairs in Col-0, *tt4-2*, *tt7-2* and *omt1*. Scale bar: 200 μm. (B) Root hair quantification of the genotypes in A. Data are mean± s.e.m. of three independent experiments (*n*=10-20 seedlings/experiment). Columns with different letters indicate statistically significant differences determined by one-way ANOVA.

levels in the transition and elongation zone, whereas maximal ROS accumulation was in the differentiation zone. There is also a striking inverse flavonol and ROS pattern across a root cross-section: flavonols and their biosynthetic enzymes are low in the epidermis, where ROS accumulate.

In *tt4* mutants, epidermal ROS levels are higher than the wild type, with trichoblast cells having the most significant increases. PO1 staining reveals a striking H_2O_2 accumulation pattern in the *tt4* mutants: *tt4* trichoblasts have significantly higher fluorescence compared with atrichoblasts and trichoblasts of Col-0. Differences in ROS accumulation between cell files is abolished by chemical complementation with naringenin or H_2O_2 scavenging by KI, with both treatments reducing root hair numbers in *tt4* to wild-type levels.

Elevated PO1 signal in trichoblasts is consistent with the localization of the ROS-producing enzyme RBOHC, where RBOHC-GFP fluorescence and *RBOHC* transcripts preferentially accumulate (Takeda et al., 2008; Brady et al., 2007). Accordingly, this PO1 pattern is absent in roots of the RBOHC mutant *rhd2-6* (Foreman et al., 2003). Additionally, the absence of IAA induction of root hairs in *rhd2-6* suggests IAA drives root hair formation by elevating ROS. This finding parallels a previous report of H_2O_2 in promoting differentiation in the primary root (Tsukagoshi et al., 2010). Together, these results suggest a positive role for RBOHC-produced ROS in initiating root hair development and for flavonols in modulating this developmental response.

Flavonols regulate other developmental processes by tissue-specific accumulation (Agati et al., 2012; Chapman et al., 2019). Longer primary roots, impaired gravitropism, and higher lateral and adventitious root numbers in multiple *tt4* alleles suggest that flavonols regulate root architecture in *Arabidopsis* (Brown et al., 2001; Buer and Djordjevic, 2009; Buer and Muday, 2004; Buer et al., 2006, 2007; Lewis et al., 2011). Localized flavonol synthesis at the root tip maintains the stem cell niche and is positively regulated by the TFs WRKY23 (Grunewald et al., 2012) and MYB12 (Lewis et al., 2011). Proper meristem development is influenced by flavonol synthesis (Grunewald et al., 2012; Silva-Navas et al., 2016), and meristem size is also regulated by superoxide/H_2O_2 gradients (Tsukagoshi et al., 2010). In tomato, reduced flavonol
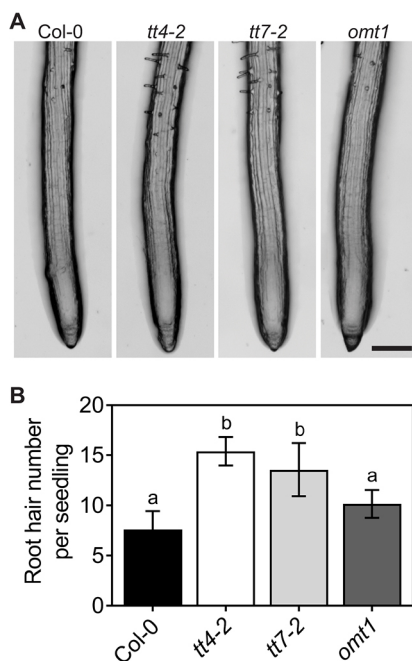
accumulation in the *are* mutant reduced lateral root development and increased root hair formation (Maloney et al., 2014). Maintenance of ROS homeostasis by flavonols also affects development and signaling in aerial tissue by regulating pavement cell and cotyledon morphology (Kuhn et al., 2011; Ringli et al., 2008), ABA-induced stomatal closure (Watkins et al., 2017), and temperature-impaired pollen grain viability and pollen tube elongation (Muhlemann et al., 2018).

Spatial control of flavonol synthesis is a key factor in regulating development. Tissue-specific flavonol synthesis is illustrated by the presence of flavonols and absence of anthocyanins in roots and pollen, which have non-detectable expression of genes producing anthocyanins (Lewis et al., 2011; Maloney et al., 2014; Muhlemann et al., 2018). Tissue-level expression of genes in the flavonol pathway is mediated by the MYB TFs MYB111 and MYB12, which control flavonol synthesis in shoots and roots, respectively (Mehrtens et al., 2005; Stracke et al., 2007). In addition, plants can locally accumulate flavonols in response to environmental signals. Directional root bending away from light exposure is driven by synthesis of *CHS* transcripts and flavonol products on the convex side of bending roots (Silva-Navas et al., 2016). Regulation of *F3′H* in the root meristem by WRKY23 drives flavonol production towards quercetin derivatives (Grunewald et al., 2012). Our studies indicate that the location of flavonol synthesis driven by CHS and FLS1 accumulation in root tissues influences ROS accumulation: high CHS, FLS1 and flavonol levels in the inner tissue layers reduces ROS, whereas low CHS and FLS1 in the epidermis allows ROS to increase to levels that stimulate root hair development.

An important question is how ROS gradients are established between trichoblast and atrichoblast cell files. We did not find differences in the fluorescence of CHS- and FLS1-GFP reporters or DPBA, between hair and non-hair cells. Similarly, there were no differences in abundance of transcripts encoding these enzymes between trichoblast and atrichoblast cells in publicly available datasets (Fucile et al., 2011; Winter et al., 2007), suggesting that these two cell types have similar flavonol levels. Yet, the absence of flavonols in the *tt4* mutants results in a striking H_2O_2 accumulation in trichoblast cells. The absence of this PO1 pattern in the *rhd2-6* mutant suggests that RBOHC leads to increased H_2O_2 synthesis and that flavonols maintain ROS homeostasis by reducing RBOHC-derived ROS in trichoblasts.

It was also important to characterize the effects of flavonols on auxin transport-regulated root development. Auxin transport from the root tip towards the shoot through the epidermal cells is an important factor in root hair elongation (Jones et al., 2002; Bhosale et al., 2018). Flavonol synthesis mutants, including several *tt4* alleles, have elevated shootward transport of radiolabeled IAA and increased signal of the auxin transcriptional reporter DR5-GUS (Buer and Muday, 2004; Lewis et al., 2011). Consistent with this, we found that *tt4-11* formed root hairs further from the root tip and showed a significant IAA induction of root hair number. Interestingly, both Col-0 and the *tt4-11* mutant showed higher PO1 levels in trichoblasts when treated with IAA, suggesting that IAA can increase ROS levels. Moreover, the lack of IAA-induced ROS accumulation in *rhd2-6* suggests that auxin-induced ROS accumulation requires the RBOHC enzyme. This result is consistent with the finding that the TF RSL4 binds to the *RBOHC* promoter in IAA-treated plants (Mangano et al., 2017). RSL4 is downstream of TFs that determine cell fate identity (Bruex et al., 2012), suggesting that an auxin-RSL4 network might be involved in ROS synthesis and root hair formation. In this scenario, flavonols may dampen root hair development by targeting both auxin transport and ROS.

What remains unknown are the targets of H_2O_2 in root hair initiation. ROS often function in signaling pathways by oxidizing cysteine residues on target proteins to cysteine sulfenic acids, a reversible process that alters protein activity (Poole and Schöneich, 2015). Flavonol and ROS accumulation in the nucleus (Lewis et al., 2011; Martins et al., 2018; Saslowsky et al., 2005) might control gene expression through cysteine oxidation of ROS-dependent TFs (LaButti et al., 2007; Pomposiello and Demple, 2001; Sivaramakrishnan et al., 2005; Viola et al., 2013, 2016). ROS can also modulate cell wall structure (Schopfer, 2001), which might allow structural changes needed for root hair formation. It is also possible that these two responses are combined to alter the cell wall chemistry directly and/or through synthesis of cell wall remodeling enzymes (Lewis et al., 2013). Accordingly, the *rhd2* mutant has altered expression of genes that affect cell wall maintenance (Bruex et al., 2012; Monshausen et al., 2007; Vissenberg et al., 2001).

These data reveal that localized flavonol antioxidants regulate ROS homeostasis to reduce root hair initiation. This leads to an important question: why do roots make flavonols if they negatively regulate development? ROS have an optimal concentration, where surpassing this level causes oxidative damage, and impaired signaling occurs below this level (Chapman et al., 2019; Schieber and Chandel, 2014). Without flavonols, plants are more sensitive to environmental stress and its negative developmental impacts, which is well documented in high temperature conditions. In tomato, flavonol synthesis results in better plant survival (Martinez et al., 2016) and decreases ROS damage to pollen and pollen tubes exposed to high temperature (Muhlemann et al., 2018). Similarly, *Arabidopsis* seedlings treated with oxidant or drought stress were protected by flavonol synthesis (Nakabayashi et al., 2014a,b). Our finding that quercetin modulates ROS and root hair development fits with the recent insight that specific flavonols and flavonol glycosides can be made in response to heat stress (Su et al., 2018). Together, these findings suggest that precise spatial, temporal and environmental controls of flavonol synthesis, help plants maintain optimal ROS levels to drive development while minimizing damage from environmental stress.

MATERIALS AND METHODS
Materials and growth conditions
All *Arabidopsis thaliana* mutants used in this study are in the Col-0 background and previously described for the following lines: *tt4-2* (Bennett et al., 2006), *tt4-11* (Buer et al., 2006) and *tt4-11* complemented with the *pCHS::CHS::GFP* transgene (Lewis et al., 2011). The *tt4-2* mutant is a backcrossed allele of *tt4*(2YY6), which contains a G-to-A mutation at the 3′ splice site in the sole intron (Bennett et al., 2006; Shirley et al., 1995), whereas *tt4-11* (SALK_020583) contains a T-DNA insertion in the second exon (Bowerman et al., 2012). Additional mutant alleles include *tt7-2* (Lewis et al., 2011), *omt1* (Tohge et al., 2007), *fls1-3* and *pFLS1::FLS1-GFP* (Kuhn et al., 2011). Out of six annotated *FLS* genes in the *Arabidopsis* genome, FLS1 and FLS3 have enzymatic activity, with FLS1 responsible for the majority of flavonol synthesis *in vivo* (Owens et al., 2008; Preuss et al., 2009).

Seeds were sterilized in 70% ethanol for 5 min and dried before sowing in a single horizontal line on 100×15 mm Petri dishes containing 30 ml of media. All plants were grown on 1× MS (Caisson Labs) supplemented with 1% sucrose, vitamins (1 µg/ml thiamine, 0.5 µg/ml pyridoxine and 0.5 µg/ml nicotinic acid), 0.05% MES (w/v, Research Products International) and 0.8% agar (MP Biomedicals). Media pH was adjusted to 5.5. The top half of the Petri dish was sealed with Micropore tape (3M) to allow gas exchange. Plated seeds were stratified at 4°C in darkness for 2-3 days to synchronize seed germination, and grown vertically under 24 h light provided by cool white fluorescent bulbs. Light intensity was 120-150 µmol photons m^{-2} s^{-1}.

DEVELOPMENT

Root hair quantification

Six-day-old seedlings were imaged under bright field using an Axio Zoom V16 stereomicroscope (Zeiss) equipped with an AxioCam 506 monochrome camera (Zeiss). Extended depth of focus was used to combine z-stack images to obtain a maximum field depth for quantification. Root hairs forming within zone 1 (1500 μm region starting at the root tip) and zone 2 (1000 μm region above zone 1) were quantified. Root hair quantification of IAA-treated seedlings is described below.

Chemical treatments

Unless otherwise indicated, seedlings were plated and grown on 1× MS media prepared as described above and 5 days old at the time of treatment. For each experiment 1× MS media were freshly prepared and cooled for 1 h in a 55-60°C water bath after autoclaving before adding chemicals. All stock solutions were freshly prepared for each experiment. Stock solutions (200 mM) of naringenin (Indofine Chemical Company) were prepared in absolute ethanol for each individual experiment and mock treatment consisted of an equal volume of absolute ethanol. Stock solutions (200 mM) of potassium iodide (Sigma-Aldrich) were dissolved in H_2O. Seedlings were transferred to control- or mock-treated media and root hair was quantified 24 h after transfer. Five-day-old Col-0 and tt4 mutants were grown on control medium and transferred to medium containing 75 μM naringenin or ethanol (mock treatment) for 24 h.

For auxin treatment, fresh stock solutions of 10 mM IAA (Sigma-Aldrich) were prepared in absolute ethanol and diluted in agar to 0.1 μM [so ethanol was diluted to 0.001% (v/v)], with mock treatments consisting of an equal concentration of ethanol. Agar (0.8%, MP Biomedicals) was dissolved in H_2O and cooled to 55-60°C before adding IAA or ethanol at the indicated concentration. Ten microliter droplets were pipetted onto Parafilm (Bemis Company) and placed in a Petri dish for 10 min to dry. Droplets containing IAA or ethanol were then placed on the primary root tip of 6-day-old seedlings, ensuring that the droplet covered the quiescent center. Root tips were imaged immediately after agar application (T0) and plates were placed under fluorescent lights with yellow filters to prevent IAA degradation. After 4 h, seedlings were imaged again (T4).

To quantify new root hairs, images of IAA- or mock-treated roots at T0 and T4 were compared. Root hairs that were present at T0 were marked and only new root hairs were counted. The dotted red line in the image is used to illustrate the most distal position of new root hairs at T4.

ROS sensor analysis

General ROS was detected using CM-H_2DCFDA (Invitrogen). Fifty micrograms of CM-H_2DCFDA was dissolved in DMSO to a concentration of 1 mM before further dilution to a working concentration of 25 μM with H_2O. Whole-seedling DCF fluorescence images in Fig. 1 were taken with an Axiozoom V16 stereomicroscope (Zeiss) equipped with a 38 (green/GFP) filter set (Zeiss) and AxioCam MRc5 full color camera (Zeiss). Whole-root images were taken immediately after application of CM-H_2DCFDA.

To examine total ROS, we incubated Col-0, tt4-2 and tt4-11 seedlings in CM-H_2DCFDA for 4 min before imaging. The short staining time was used to maximize DCF signal in the epidermis and avoid dye quenching and photoactivation, which can occur with longer staining times and in response to extended imaging, respectively (Winterbourn, 2014). For quantification of ROS in the epidermis, seedlings were mounted in CM-H_2DCFDA onto microscope slides and incubated for 4 min in darkness before imaging. Because fluorescence depends on CM-H_2DCFDA uptake and interaction with ROS, no washes were performed after incubation in the dye. Fluorescence was detected using a Zeiss LSM 880 confocal microscope with a 3% laser power of 488 nm, and the pinhole set at 1 Airy unit. For each root, z-stack images were generated using 10× objective with a line averaging set at 2. To verify that mutations had no effect on dye uptake, fluorescein diacetate (FDA, ACROS Organics) controls were performed. FDA was diluted and imaged in the same manner as CH-H_2DCFDA.

H_2O_2 levels in the epidermis were imaged with Peroxy Orange 1 (PO1, Tocris). PO1 was dissolved to make a 500 μM stock solution with DMSO before further dilution with H_2O to make a working concentration of 50 μM. Seedlings were incubated in PO1 for 15 min in darkness and briefly rinsed and mounted in H_2O for imaging. Fluorescence was excited using a 488 nm

laser at 0.25% power with a pinhole setting of 1 Airy unit, and emission was captured between 544-695 nm. All microscope settings described above were identical when analyzing each biological experiment. Figures are representative images of optical slices of the median section of the root, or maximum intensity projections.

Fiji software (Schindelin et al., 2012) was used to measure and generate plot profiles for DCF, FDA and PO1 fluorescence intensity. Plot profiles were measured from the central longitudinal section of the root using segmented lines set to a width of 12 pixels to trace a 1500 μm region of the epidermis starting at the tip. Average total fluorescence was determined by averaging values within the 1500 μm region of the epidermis. Fluorescence intensity across epidermal cell files at the surface of the root was measured using a 20 pixel-wide line and averaging the values within each epidermal file. To generate the heat maps in Fig. 1, pixel intensities of images of DCF fluorescence were converted using the look-up tables (LUT) function in Fiji. The fluorescence intensity scale in Fig. 1 represents the minimum and maximum fluorescence of 16-bit images of 0 ('low') and 65,536 ('high'), whereas 8-bit images in Fig. 2 have a minimum of 0 and maximum of 255. In Fig. 1 the image shows the LUT with samples that are at normal settings without saturation and saturated images, as tt4 has much higher fluorescence making it difficult to see the tip-focused DCF gradient in Col-0.

DPBA staining

We analyzed the localization patterns of flavonols in Col-0 roots using the probe DPBA (Sheahan and Rechnitz, 1992). DPBA fluoresces upon binding to quercetin and kaempferol as either free aglycones or flavonol glycosides but does not bind to isorhamnetin or its conjugates in vitro and in vivo (Lewis et al., 2011; Peer et al., 2001). In vivo fluorescence differs between kaempferol DPBA (green shifted) and quercetin-DPBA (yellow shifted), allowing distinct visualization of these two flavonols (and the glycosylated conjugates) by LSCM (Lewis et al., 2011). The specificity of this dye was verified by staining the tt4-2 and tt7-2 mutants (Lewis et al., 2011). The tt4-2 mutant lacked a DPBA signal, whereas tt7-2 only had the kaempferol-DPBA signal, which is shifted to green wavelengths and shown in our images as green. To obtain emission spectra specific to quercetin, the tt4-2 mutant was treated with quercetin, which revealed that the quercetin-DPBA signal was shifted to yellow and is shown as yellow in our images.

For the visualization of quercetin and kaempferol in vivo, seedlings were stained in 0.25% w/v DPBA (Sigma-Aldrich), which was dissolved in 0.06% Triton-X (v/v) in water. Seedlings were incubated in DPBA dye for 7 min and then incubated in H_2O for 7 min in darkness. Roots were imaged using a Zeiss LSM 880 confocal microscope and 25% laser power at 458. The pinhole was set to 1 Airy scan unit and emission spectra were captured for kaempferol-bound DPBA (475-500 nm) and quercetin-bound DPBA (585-619 nm). z-stack images were taken using a 10× objective and images were analyzed from the center longitudinal section or as maximum intensity projections. All microscope settings described above were identical when analyzing each biological experiment. To represent fluorescence intensity of quercetin and kaempferol as a heat map, pixel intensities of images of DPBA-stained seedlings were converted to LUT function using Fiji software. The fluorescence intensity scale represents the minimum and maximum fluorescence of 8-bit images of 0 ('low') and 255 ('high'), respectively.

Nuclear localization of quercetin-DPBA was verified using Hoechst 34580 dye (Invitrogen). Stock solutions of 500 μg/ml were made with water before further dilution to 5 μg/ml in 0.06% Triton X-100 (v/v). Seedlings were first immersed in DPBA solution for 45 min before transfer to Hoechst 34580 dye for 10 min. Fluorescence of Hoechst 34580 dye and quercetin-bound DPBA in the root was visualized concurrently by confocal microscopy. Hoechst 34580 dye fluorescence was probed using a 405 nm laser at 1.3% power and emission captured between 410 and 450 nm. Quercetin-bound DPBA was visualized using a 458 nm laser at 5% power and emission captured between 585 and 619 nm.

Localization of CHS-GFP and FLS1-GFP

Six-day-old transgenic seedlings harboring the pCHS::CHS::GFP or pFLS1::FLS1-GFP transgene were mounted in H_2O and excited with a 488 nm laser at 5% and emission collected between 490 and 544 nm. The presence or absence of CHS-GFP and FLS1-GFP signal in the epidermis

DEVELOPMENT

was determined by increasing laser power to saturate GFP fluorescence in the inner tissues. Cell walls were stained with 0.5 μg ml^{-1} propidium iodide (PI, Acros Organics) dissolved in H$_2$O. Seedlings were incubated in PI for 9 min before visualization of PI fluorescence using a 561 nm laser at 0.25% and emission spectra set to 570-735 nm. All microscope settings described above were identical when analyzing each biological experiment. Optical sections of the median section of the root, or maximum intensity projections of z-stack images are shown in the figures.

Flavonol extraction and quantification by liquid chromatography-mass spectrometry

Flavonols were extracted as described previously (Maloney et al., 2014). Briefly, roots and shoots of 6-day-old seedlings were separated and flash frozen in liquid nitrogen or immediately used for extraction. Extraction buffer consisted of an internal standard of 500 nM formononetin (Indofine Chemical Company) in 100% acetone (v/v, Optima grade, Fisher Scientific) and was added to samples at 3 μl/mg. Tissues were homogenized using a 1600 MiniG tissue homogenizer (Spex SamplePrep) and were incubated in extraction buffer in darkness at 4°C overnight. An equal volume of 2 N HCl was added and samples were incubated at 75°C for 2 h to produce aglycone flavonols. An equal volume of ethyl acetate (Optima grade, Fisher Scientific) was added and shaken for 1 min before centrifugation at 16,800 g for 10 min. The top organic phase was isolated and dried by airflow using a Mini-Vap evaporator (Supelco). Samples were resuspended in 150-300 μl of acetone (Optima grade, Fisher Scientific) before analysis.

Flavonol levels were quantified using a Thermo Orbitrap LTQ XL high-resolution mass spectrometer equipped with a Thermo Accela 1250 liquid chromatograph and autosampler (Thermo Fisher Scientific). Samples were separated on a Luna 3 μm C18(2) 100 Å 150×3 mm column (Phenomenex) equipped with a HLPC security guard cartridge (Phenomenex). Ten microliters of sample were injected into a water/acetonitrile solvent system, both containing 0.1% formic acid, at gradient percentages (in v/v) of 90/10 from 0 to 18.5 min, 10/90 from 18.5 to 20 min, and 90/10 from 20 to 22 min in positive ion mode, with a scan range of 200-600 m/z. Peak areas of individual aglycone flavonols were extracted from the chromatogram using Thermo Xcalibur software and converted to μmol using standard curves of known amounts of pure naringenin, quercetin, kaempferol and isorhamnetin compounds (Indofine Chemical Company). Flavonol concentrations were then normalized to the mass of tissue used in the extraction.

Statistical analysis

Analysis of variance (ANOVA) of quantified data was determined using the GraphPad Prism 7 software package. ANOVA analyses in Figs 4-8 and Fig. 10 were followed by Tukey's multiple comparison test, for which significance was defined as $P<0.05$.

Author contributions
Conceptualization: S.R.G., G.K.M.; Methodology: S.R.G.; Investigation: S.R.G.; Writing - original draft: S.R.G.; Writing - review & editing: S.R.G., G.K.M.; Supervision: G.K.M.; Project administration: G.K.M.; Funding acquisition: G.K.M.

References

Agati, G. and Tattini, M. (2010). Multiple functional roles of flavonoids in photoprotection. *New Phytol.* **186**, 786-793. doi:10.1111/j.1469-8137.2010.03269.x

Agati, G., Azzarello, E., Pollastri, S. and Tattini, M. (2012). Flavonoids as antioxidants in plants: location and functional significance. *Plant Sci.* **196**, 67-76. doi:10.1016/j.plantsci.2012.07.014

Bennett, T., Sieberer, T., Willett, B., Booker, J., Luschnig, C. and Leyser, O. (2006). The Arabidopsis MAX pathway controls shoot branching by regulating auxin transport. *Curr. Biol.* **16**, 553-563. doi:10.1016/j.cub.2006.01.058

Bernhardt, C., Lee, M. M., Gonzalez, A., Zhang, F., Lloyd, A. and Schiefelbein, J. (2003). The bHLH genes GLABRA3 (GL3) and ENHANCER OF GLABRA3 (EGL3) specify epidermal cell fate in the Arabidopsis root. *Development* **130**, 6431-6439. doi:10.1242/dev.00880

Bhosale, R., Giri, J., Pandey, B. K., Giehl, R. F. H., Hartmann, A., Traini, R., Truskina, J., Leftley, N., Hanlon, M., Swarup, K. et al. (2018). A mechanistic framework for auxin dependent *Arabidopsis* root hair elongation to low external phosphate. *Nat. Comm.* **9**, 1409. doi:10.1038/s41467-018-03851-3

Bowerman, P. A., Ramirez, M. V., Price, M. B., Helm, R. F. and Winkel, B. S. J. (2012). Analysis of T-DNA alleles of flavonoid biosynthesis genes in Arabidopsis ecotype Columbia. *BMC Research Notes* **5**, 485. doi:10.1186/1756-0500-5-485

Brady, S. M., Orlando, D. A., Lee, J.-Y., Wang, J. Y., Koch, J., Dinneny, J. R., Mace, D., Ohler, U. and Benfey, P. N. (2007). A high-resolution root spatiotemporal map reveals dominant expression patterns. *Science* **318**, 801-806. doi:10.1126/science.1146265

Brown, D. E., Rashotte, A. M., Murphy, A. S., Normanly, J., Tague, B. W., Peer, W. A., Taiz, L. and Muday, G. K. (2001). Flavonoids act as negative regulators of auxin transport in vivo in arabidopsis. *Plant Physiol.* **126**, 524-535. doi:10.1104/pp.126.2.524

Bruex, A., Kainkaryam, R. M., Wieckowski, Y., Kang, Y. H., Bernhardt, C., Xia, Y., Zheng, X., Wang, J. Y., Lee, M. M., Benfey, P. et al. (2012). A gene regulatory network for root epidermis cell differentiation in Arabidopsis. *PLoS Genet.* **8**, e1002446. doi:10.1371/journal.pgen.1002446

Buer, C. S. and Djordjevic, M. A. (2009). Architectural phenotypes in the transparent testa mutants of Arabidopsis thaliana. *J. Exp. Bot.* **60**, 751-763. doi:10.1093/jxb/ern323

Buer, C. S. and Muday, G. K. (2004). The transparent testa4 mutation prevents flavonoid synthesis and alters auxin transport and the response of Arabidopsis roots to gravity and light. *Plant Cell* **16**, 1191-1205. doi:10.1105/tpc.020313

Buer, C. S., Sukumar, P. and Muday, G. K. (2006). Ethylene modulates flavonoid accumulation and gravitropic responses in roots of Arabidopsis. *Plant Physiol.* **140**, 1384-1396. doi:10.1104/pp.105.075671

Buer, C. S., Muday, G. K. and Djordjevic, M. A. (2007). Flavonoids are differentially taken up and transported long distances in Arabidopsis. *Plant Physiol.* **145**, 478-490. doi:10.1104/pp.107.101824

Carol, R. J., Takeda, S., Linstead, P., Durrant, M. C., Kakesova, H., Derbyshire, P., Drea, S., Zarsky, V. and Dolan, L. (2005). A RhoGDP dissociation inhibitor spatially regulates growth in root hair cells. *Nature* **438**, 1013-1016. doi:10.1038/nature04198

Chapman, J. M., Muhlemann, J. K., Gayomba, S. R. and Muday, G. K. (2019). RBOH-dependent ROS synthesis and ROS scavenging by plant specialized metabolites to modulate plant development and stress responses. *Chem. Res. Toxicol.* **32**, 370-396. doi:10.1021/acs.chemrestox.9b00028

Dickinson, B. C., Huynh, C. and Chang, C. J. (2010). A palette of fluorescent probes with varying emission colors for imaging hydrogen peroxide signaling in living cells. *J. Am. Chem. Soc.* **132**, 5906-5915. doi:10.1021/ja1014103

Dindas, J., Scherzer, S., Roelfsema, M. R. G., von Meyer, K., Muller, H. M., Al-Rasheid, K. A. S., Palme, K., Dietrich, P., Becker, D., Bennett, M. J. et al. (2018). AUX1-mediated root hair auxin influx governs SCFTIR1/AFB-type Ca2$^+$ signaling. *Nat. Comm.* **9**, 1174. doi:10.1038/s41467-018-03582-5

Duckett, C. M., Grierson, C., Linstead, P., Schneider, K., Lawson, E., Dean, C., Poethig, S. and Roberts, K. (1994). Clonal relationships and cell patterning in the root epidermis of Arabidopsis. *Development* **120**, 2465-2474.

Dunand, C., Crèvecoeur, M. and Penel, C. (2007). Distribution of superoxide and hydrogen peroxide in Arabidopsis root and their influence on root development: possible interaction with peroxidases. *New Phytol.* **174**, 332-341. doi:10.1111/j.1469-8137.2007.01995.x

Feng, Y., Xu, P., Li, B., Li, P., Wen, X., An, F., Gong, Y., Xin, Y., Zhu, Z., Wang, Y. et al. (2017). Ethylene promotes root hair growth through coordinated EIN3/EIL1 and RHD6/RSL1 activity in Arabidopsis. *Proc. Natl. Acad. Sci. USA* **114**, 13834-13839. doi:10.1073/pnas.1711723115

Fernández-Marcos, M., Sanz, L., Lewis, D. R., Muday, G. K. and Lorenzo, O. (2013). Control of auxin transport by reactive oxygen and nitrogen species. In *Polar Auxin Transport* (ed. R. Chen and F. Baluška), pp. 103-117. Berlin, Heidelberg: Springer Berlin Heidelberg.

Foreman, J., Demidchik, V., Bothwell, J. H. F., Mylona, P., Miedema, H., Torres, M. A., Linstead, P., Costa, S., Brownlee, C., Jones, J. D. G. et al. (2003). Reactive oxygen species produced by NADPH oxidase regulate plant cell growth. *Nature* **422**, 442-446. doi:10.1038/nature01485

Forkmann, G., de Vlaming, P., Spribille, R., Wiering, H. and Schram, A. W. (1986). Genetic and biochemical studies on the conversion of dihydroflavonols to flavonols and anthocyanins in flowers of Petunia hybrida. *Planta* 179-186. doi:10.1515/znc-1986-1-227

DEVELOPMENT

Fucile, G., Biase, D. D., Nahal, H., La, G., Khodabandeh, S., Chen, Y., Easley, K., Christendat, D., Kelley, L. and Provart, N. J. (2011). ePlant and the 3D data display initiative: integrative systems biology on the world wide web. *PLoS ONE* **6**, e15237. doi:10.1371/journal.pone.0015237

Gayomba, S. R., Watkins, J. M. and Muday, G. K. (2016). Flavonols regulate plant growth and development through regulation of auxin transport and cellular redox status. In *Recent Advances in Polyphenol Research* (ed. K. Yoshida, V. Cheynier and S. Quideau), pp. 143-170. John Wiley & Sons, Ltd.

Giehl, R. F. H. and von Wirén, N. (2014). Root nutrient foraging. *Plant Physiol.* **166**, 509-517. doi:10.1104/pp.114.245225

Grunewald, W., De Smet, I., Lewis, D. R., Löfke, C., Jansen, L., Goeminne, G., Vanden Bossche, R., Karimi, M., De Rybel, B., Vanholme, B. et al. (2012). Transcription factor WRKY23 assists auxin distribution patterns during Arabidopsis root development through local control on flavonol biosynthesis. *Proc. Natl. Acad. Sci. USA* **109**, 1554-1559. doi:10.1073/pnas.1121134109

Holton, T. A., Brugliera, F. and Tanaka, Y. (1993). Cloning and expression of flavonol synthase from Petunia hybrida. *Plant J.* **4**, 1003-1010. doi:10.1046/j.1365-313X.1993.04061003.x

Jiang, K., Meng, Y. L. and Feldman, L. J. (2003). Quiescent center formation in maize roots is associated with an auxin-regulated oxidizing environment. *Development* **130**, 1429-1438. doi:10.1242/dev.00359

Jones, M. A., Shen, J.-J., Fu, Y., Li, H., Yang, Z. and Grierson, C. S. (2002). The Arabidopsis Rop2 GTPase is a positive regulator of both root hair initiation and tip growth. *Plant Cell* **14**, 763-776. doi:10.1105/tpc.010359

Jones, M. A., Raymond, M. J., Yang, Z. and Smirnoff, N. (2007). NADPH oxidase-dependent reactive oxygen species formation required for root hair growth depends on ROP GTPase. *J. Exp. Bot.* **58**, 1261-1270. doi:10.1093/jxb/erl279

Joo, J. H., Bae, Y. S. and Lee, J. S. (2001). Role of auxin-induced reactive oxygen species in root gravitropism. *Plant Physiol.* **126**, 1055-1060. doi:10.1104/pp.126.3.1055

Kwasniewski, M., Nowakowska, U., Szumera, J., Chwialkowska, K. and Szarejko, I. (2013). iRootHair: a comprehensive root hair genomics database. *Plant Physiol.* **161**, 28-35. doi:10.1104/pp.112.206441

Kwasniewski, M., Daszkowska-Golec, A., Janiak, A., Chwialkowska, K., Nowakowska, U., Sablok, G. and Szarejko, I. (2016). Transcriptome analysis reveals the role of the root hairs as environmental sensors to maintain plant functions under water-deficiency conditions. *J. Exp. Bot.* **67**, 1079-1094. doi:10.1093/jxb/erv498

Kim, J., Lee, W. J., Vu, T. T., Jeong, C. Y., Hong, S.-W. and Lee, H. (2017). High accumulation of anthocyanins via the ectopic expression of AtDFR confers significant salt stress tolerance in Brassica napus L. *Plant Cell Rep.* **36**, 1215-1224. doi:10.1007/s00299-017-2147-7

Koornneef, M. (1990). Mutations affecting the testa color in Arabidopsis. *Arabidopsis Information Services* **27**,1-4.

Kuhn, B. M., Geisler, M., Bigler, L. and Ringli, C. (2011). Flavonols accumulate asymmetrically and affect auxin transport in Arabidopsis1. *Plant Physiol.* **156**, 585-595. doi:10.1104/pp.111.175976

LaButti, J. N., Chowdhury, G., Reilly, T. J. and Gates, K. S. (2007). Redox regulation of protein tyrosine phosphatase 1B (PTP1B) by Peroxymonophosphate (=O3POOH). *J. Am. Chem. Soc.* **129**, 5320. doi:10.1021/ja070194j

Lee, M. M. and Schiefelbein, J. (1999). WEREWOLF, a MYB-related protein in Arabidopsis, is a position-dependent regulator of epidermal cell patterning. *Cell* **99**, 473-483. doi:10.1016/S0092-8674(00)81536-6

Lee, Y., Rubio, M. C., Alassimone, J. and Geldner, N. (2013). A mechanism for localized lignin deposition in the endodermis. *Cell* **153**, 402-412. doi:10.1016/j.cell.2013.02.045

Lewis, D. R., Miller, N. D., Splitt, B. L., Wu, G. and Spalding, E. P. (2007). Separating the roles of acropetal and basipetal auxin transport on gravitropism with mutations in two Arabidopsis multidrug resistance-like ABC transporter genes. *Plant Cell* **19**, 1838-1850. doi:10.1105/tpc.107.051599

Lewis, D. R., Ramirez, M. V., Miller, N. D., Vallabhaneni, P., Ray, W. K., Helm, R. F., Winkel, B. S. J. and Muday, G. K. (2011). Auxin and ethylene induce flavonol accumulation through distinct transcriptional networks. *Plant Physiol.* **156**, 144-164. doi:10.1104/pp.111.172502

Lewis, D. R., Olex, A. L., Lundy, S. R., Turkett, W. H., Fetrow, J. S. and Muday, G. K. (2013). A kinetic of the auxin transcriptome reveals cell wall remodeling proteins that modulate lateral root development in Arabidopsis. *Plant Cell* **25**, 3329-3346. doi:10.1105/tpc.113.114868

Liebhafsky, H. A. (1934). The catalytic decomposition of hydrogen peroxide by the iodine—iodide couple. IV. The approach to the steady state[1]. *J. Am. Chem. Soc.* **56**, 2369-2372. doi:10.1021/ja01326a043

Lin, Q., Ohashi, Y., Kato, M., Tsuge, T., Gu, H., Qu, L.-J. and Aoyama, T. (2015). GLABRA2 directly suppresses basic helix-loop-helix transcription factor genes with diverse functions in root hair development. *Plant Cell* **27**, 2894-2906. doi:10.1105/tpc.15.00607

Maloney, G. S., DiNapoli, K. T. and Muday, G. K. (2014). The anthocyanin reduced tomato mutant demonstrates the role of flavonols in tomato lateral root and root hair development. *Plant Physiol.* **166**, 614-631. doi:10.1104/pp.114.240507

Mangano, S., Denita-Juarez, S. P., Choi, H.-S., Marzol, E., Hwang, Y., Ranocha, P., Velasquez, S. M., Borassi, C., Barberini, M. L., Aptekmann, A. A. et al.

(2017). Molecular link between auxin and ROS-mediated polar growth. *Proc. Natl. Acad. Sci. USA* **114**, 5289-5294. doi:10.1073/pnas.1701536114

Martinez, V., Mestre, T. C., Rubio, F., Girones-Vilaplana, A., Moreno, D. A., Mittler, R. and Rivero, R. M. (2016). Accumulation of flavonols over hydroxycinnamic acids favors oxidative damage protection under abiotic stress. *Front. Plant Sci.* **7**, 838. doi:10.3389/fpls.2016.00838

Martins, L., Trujillo-Hernandez, J. A. and Reichheld, J.-P. (2018). Thiol based redox signaling in plant nucleus. *Front. Plant Sci.* **9**, 705. doi:10.3389/fpls.2018.00705

Masucci, J. D., Rerie, W. G., Foreman, D. R., Zhang, M., Galway, M. E., Marks, M. D. and Schiefelbein, J. W. (1996). The homeobox gene GLABRA2 is required for position-dependent cell differentiation in the root epidermis of Arabidopsis thaliana. *Development* **122**, 1253-1260.

Mehrtens, F., Kranz, H., Bednarek, P. and Weisshaar, B. (2005). The arabidopsis transcription factor MYB12 is a flavonol-specific regulator of phenylpropanoid biosynthesis. *Plant Physiol.* **138**, 1083-1096. doi:10.1104/pp.104.058032

Mittler, R., Vanderauwera, S., Suzuki, N., Miller, G., Tognetti, V. B., Vandepoele, K., Gollery, M., Shulaev, V. and Van Breusegem, F. (2011). ROS signaling: the new wave? *Trends Plant Sci.* **16**, 300-309. doi:10.1016/j.tplants.2011.03.007

Monshausen, G. B., Bibikova, T. N., Messerli, M. A., Shi, C. and Gilroy, S. (2007). Oscillations in extracellular pH and reactive oxygen species modulate tip growth of Arabidopsis root hairs. *Proc. Natl. Acad. Sci. USA* **104**, 20996-21001. doi:10.1073/pnas.0708586104

Muhlemann, J. K., Younts, T. L. B. and Muday, G. K. (2018). Flavonols control pollen tube growth and integrity by regulating ROS homeostasis during high-temperature stress. *Proc. Natl. Acad. Sci. USA* **115**, E11188-E11197. doi:10.1073/pnas.1811492115

Müller, M. and Schmidt, W. (2004). Environmentally induced plasticity of root hair development in Arabidopsis. *Plant Physiol.* **134**, 409-419. doi:10.1104/pp.103.029066

Murphy, A., Peer, W. A. and Taiz, L. (2000). Regulation of auxin transport by aminopeptidases and endogenous flavonoids. *Planta* **211**, 315-324. doi:10.1007/s004250000300

Muzac, I., Wang, J., Anzellotti, D., Zhang, H. and Ibrahim, R. K. (2000). Functional expression of an Arabidopsis cDNA clone encoding a flavonol 3′-O-methyltransferase and characterization of the gene product. *Arch. Biochem. Biophys.* **375**, 385-388. doi:10.1006/abbi.1999.1681

Nakabayashi, R., Mori, T. and Saito, K. (2014a). Alternation of flavonoid accumulation under drought stress in Arabidopsis thaliana. *Plant Signal Behav.* **9**, e29518. doi:10.4161/psb.29518

Nakabayashi, R., Yonekura-Sakakibara, K., Urano, K., Suzuki, M., Yamada, Y., Nishizawa, T., Matsuda, F., Kojima, M., Sakakibara, H., Shinozaki, K. et al. (2014b). Enhancement of oxidative and drought tolerance in Arabidopsis by overaccumulation of antioxidant flavonoids. *Plant J.* **77**, 367-379. doi:10.1111/tpj.12388

Orman-Ligeza, B., Parizot, B., de Rycke, R., Fernandez, A., Himschoot, E., Van Breusegem, F., Bennett, M. J., Périlleux, C., Beeckman, T. and Draye, X. (2016). RBOH-mediated ROS production facilitates lateral root emergence in Arabidopsis. *Development* **143**, 3328-3339. doi:10.1242/dev.136465

Owens, D. K., Alerding, A. B., Crosby, K. C., Bandara, A. B., Westwood, J. H. and Winkel, B. S. J. (2008). Functional analysis of a predicted flavonol synthase gene family in arabidopsis. *Plant Physiol.* **147**, 1046-1061. doi:10.1104/pp.108.117457

Peer, W. A., Brown, D. E., Tague, B. W., Muday, G. K., Taiz, L. and Murphy, A. S. (2001). Flavonoid accumulation patterns of transparent testa mutants of Arabidopsis. *Plant Physiol.* **126**, 536-548. doi:10.1104/pp.126.2.536

Peer, W. A., Bandyopadhyay, A., Blakeslee, J. J., Makam, S. N., Chen, R. J., Masson, P. H. and Murphy, A. S. (2004). Variation in expression and protein localization of the PIN family of auxin efflux facilitator proteins in flavonoid mutants with altered auxin transport in arabidopsis thaliana. *Plant Cell* **16**, 1898-1911. doi:10.1105/tpc.021501

Peer, W. A., Cheng, Y. and Murphy, A. S. (2013). Evidence of oxidative attenuation of auxin signalling. *J. Exp. Bot.* **64**, 2629-2639. doi:10.1093/jxb/ert152

Pomposiello, P. J. and Demple, B. (2001). Redox-operated genetic switches: the SoxR and OxyR transcription factors. *Trends Biotechnol.* **19**, 109-114. doi:10.1016/S0167-7799(00)01542-0

Poole, L. B. and Schöneich, C. (2015). Introduction: what we do and do not know regarding redox processes of thiols in signaling pathways. *Free Radic. Biol. Med.* **80**, 145-147. doi:10.1016/j.freeradbiomed.2015.02.005

Preuss, A., Stracke, R., Weisshaar, B., Hillebrecht, A., Matern, U. and Martens, S. (2009). Arabidopsis thaliana expresses a second functional flavonol synthase. *FEBS Lett.* **583**, 1981-1986. doi:10.1016/j.febslet.2009.05.006

Ray, P. D., Huang, B.-W. and Tsuji, Y. (2012). Reactive oxygen species (ROS) homeostasis and redox regulation in cellular signaling. *Cell. Signal.* **24**, 981-990. doi:10.1016/j.cellsig.2012.01.008

Ringli, C., Bigler, L., Kuhn, B. M., Leiber, R.-M., Diet, A., Santelia, D., Frey, B., Pollmann, S. and Klein, M. (2008). The modified flavonol glycosylation profile in the Arabidopsis rol1 mutants results in alterations in plant growth and cell shape formation. *Plant Cell* **20**, 1470-1481. doi:10.1105/tpc.107.053249

Rotman, B. and Papermaster, B. W. (1966). Membrane properties of living mammalian cells as studied by enzymatic hydrolysis of fluorogenic esters. *Proc. Natl. Acad. Sci. USA* **55**, 134-141. doi:10.1073/pnas.55.1.134

Salazar-Henao, J. E., Vélez-Bermúdez, I. C. and Schmidt, W. (2016). The regulation and plasticity of root hair patterning and morphogenesis. *Development* **143**, 1848-1858. doi:10.1242/dev.132845

Saslowsky, D. E., Warek, U. and Winkel, B. S. J. (2005). Nuclear localization of flavonoid enzymes in Arabidopsis. *J. Biol. Chem.* **280**, 23735-23740. doi:10.1074/jbc.M413506200

Schieber, M. and Chandel, N. S. (2014). ROS function in redox signaling and oxidative stress. *Curr. Biol.* **24**, R453-R462. doi:10.1016/j.cub.2014.03.034

Schiefelbein, J. W. and Somerville, C. (1990). Genetic control of root hair development in Arabidopsis thaliana. *Plant Cell* **2**, 235-243. doi:10.2307/3869138

Schindelin, J., Arganda-Carreras, I., Frise, E., Kaynig, V., Longair, M., Pietzsch, T., Preibisch, S., Rueden, C., Saalfeld, S., Schmid, B. et al. (2012). Fiji: an open-source platform for biological-image analysis. *Nat. Methods* **9**, 676-682. doi:10.1038/nmeth.2019

Schoenbohm, C., Martens, S., Eder, C., Forkmann, G. and Weisshaar, B. (2000). Identification of the Arabidopsis thaliana flavonoid 3′-hydroxylase gene and functional expression of the encoded P450 enzyme. *Biol. Chem.* **381**, 749-753. doi:10.1515/BC.2000.095

Schopfer, P. (2001). Hydroxyl radical-induced cell-wall loosening in vitro and in vivo: implications for the control of elongation growth. *Plant J.* **28**, 679-688. doi:10.1046/j.1365-313x.2001.01187.x

Sheahan, J. J. and Rechnitz, G. A. (1992). Flavonoid-specific staining of Arabidopsis thaliana. *BioTechniques* **13**, 880-883.

Shirley, B. W., Kubasek, W. L., Storz, G., Bruggemann, E., Koornneef, M., Ausubel, F. M. and Goodman, H. M. (1995). Analysis of Arabidopsis mutants deficient in flavonoid biosynthesis. *Plant J.* **8**, 659-671. doi:10.1046/j.1365-313X.1995.08050659.x

Silva-Navas, J., Moreno-Risueno, M. A., Manzano, C., Téllez-Robledo, B., Navarro-Neila, S., Carrasco, V., Pollmann, S., Gallego, F. J. and del Pozo, J. C. (2016). Flavonols mediate root phototropism and growth through regulation of proliferation-to-differentiation transition. *Plant Cell* **28**, 1372-1387. doi:10.1105/tpc.15.00857

Sivaramakrishnan, S., Keerthi, K. and Gates, K. S. (2005). A chemical model for redox regulation of protein tyrosine phosphatase 1B (PTP1B) activity. *J. Am. Chem. Soc.* **127**, 10830-10831. doi:10.1021/ja052599e

Stracke, R., Ishihara, H., Huep, G., Barsch, A., Mehrtens, F., Niehaus, K. and Weisshaar, B. (2007). Differential regulation of closely related R2R3-MYB transcription factors controls flavonol accumulation in different parts of the Arabidopsis thaliana seedling. *Plant J.* **50**, 660-677. doi:10.1111/j.1365-313X.2007.03078.x

Su, X., Wang, W., Xia, T., Gao, L., Shen, G. and Pang, Y. (2018). Characterization of a heat responsive UDP: Flavonoid glucosyltransferase gene in tea plant (Camellia sinensis). *PLoS ONE* **13**, e0207212. doi:10.1371/journal.pone.0207212

Takeda, S., Gapper, C., Kaya, H., Bell, E., Kuchitsu, K. and Dolan, L. (2008). Local positive feedback regulation determines cell shape in root hair cells. *Science* **319**, 1241-1244. doi:10.1126/science.1152505

Tanimoto, M., Roberts, K. and Dolan, L. (1995). Ethylene is a positive regulator of root hair development in Arabidopsis thaliana. *Plant J.* **8**, 943-948. doi:10.1046/j.1365-313X.1995.8060943.x

Teng, S., Keurentjes, J., Bentsink, L., Koornneef, M. and Smeekens, S. (2005). Sucrose-specific induction of anthocyanin biosynthesis in Arabidopsis requires the MYB75/PAP1 gene. *Plant Physiol.* **139**, 1840-1852. doi:10.1104/pp.105.066688

Tohge, T., Yonekura-Sakakibara, K., Niida, R., Watanabe-Takahashi, A. and Saito, K. (2007). Phytochemical genomics in Arabidopsis thaliana: a case study for functional identification of flavonoid biosynthesis genes. *Pure Appl. Chem.* **79**, 811-823. doi:10.1351/pac200779040811

Tsukagoshi, H., Busch, W. and Benfey, P. N. (2010). Transcriptional regulation of ROS controls transition from proliferation to differentiation in the root. *Cell* **143**, 606-616. doi:10.1016/j.cell.2010.10.020

Verbelen, J.-P., De Cnodder, T., Le, J., Vissenberg, K. and Baluška, F. (2006). The root apex of arabidopsis thaliana consists of four distinct zones of growth activities. *Plant Signal Behav.* **1**, 296-304. doi:10.4161/psb.1.6.3511

Viola, I. L., Güttlein, L. N. and Gonzalez, D. H. (2013). Redox modulation of plant developmental regulators from the class I TCP transcription factor family. *Plant Physiol.* **162**, 1434-1447. doi:10.1104/pp.113.216416

Viola, I. L., Camoirano, A. and Gonzalez, D. H. (2016). Redox-dependent modulation of anthocyanin biosynthesis by the TCP transcription factor TCP15 during exposure to high light intensity conditions in Arabidopsis. *Plant Physiol.* **170**, 74-85. doi:10.1104/pp.15.01016

Vissenberg, K., Fry, S. C. and Verbelen, J.-P. (2001). Root hair initiation is coupled to a highly localized increase of Xyloglucan Endotransglycosylase action in arabidopsis roots. *Plant Physiol.* **127**, 1125-1135. doi:10.1104/pp.010295

Wada, T., Tachibana, T., Shimura, Y. and Okada, K. (1997). Epidermal cell differentiation in *Arabidopsis* determined by a *Myb* homolog, *CPC*. *Science* **277**, 1113-1116. doi:10.1126/science.277.5329.1113

Walker, A. R., Davison, P. A., Bolognesi-Winfield, A. C., James, C. M., Srinivasan, N., Blundell, T. L., Esch, J. J., Marks, M. D. and Gray, J. C. (1999). The TRANSPARENT TESTA GLABRA1 locus, which regulates trichome differentiation and anthocyanin biosynthesis in Arabidopsis, encodes a WD40 repeat protein. *Plant Cell* **11**, 1337-1349. doi:10.1105/tpc.11.7.1337

Watanabe, S., Sato, M., Sawada, Y., Tanaka, M., Matsui, A., Kanno, Y., Hirai, M. Y., Seki, M., Sakamoto, A. and Seo, M. (2018). Arabidopsis molybdenum cofactor sulfurase ABA3 contributes to anthocyanin accumulation and oxidative stress tolerance in ABA-dependent and independent ways. *Sci. Rep.* **8**, 16592. doi:10.1038/s41598-018-34862-1

Watkins, J. M., Hechler, P. J. and Muday, G. K. (2014). Ethylene-induced flavonol accumulation in guard cells suppresses reactive oxygen species and moderates stomatal aperture. *Plant Physiol.* **164**, 1707-1717. doi:10.1104/pp.113.233528

Watkins, J. M., Chapman, J. M. and Muday, G. K. (2017). Abscisic acid-induced reactive oxygen species are modulated by flavonols to control stomata aperture. *Plant Physiol.* **175**, 1807-1825. doi:10.1104/pp.17.01010

Winter, D., Vinegar, B., Nahal, H., Ammar, R., Wilson, G. V. and Provart, N. J. (2007). An "electronic fluorescent pictograph" browser for exploring and analyzing large-scale biological data sets. *PLoS ONE* **2**, e718. doi:10.1371/journal.pone.0000718

Winterbourn, C. C. (2014). The challenges of using fluorescent probes to detect and quantify specific reactive oxygen species in living cells. *Biochim. Biophys. Acta* **1840**, 730-738. doi:10.1016/j.bbagen.2013.05.004